

Original Articles

Spatiotemporal variations and the driving factors of PM_{2.5} in Xi'an, China between 2004 and 2018

Abula Tuheti ^{a,b}, Shunxi Deng ^{a,b,*}, Jianghao Li ^{a,b}, Guanghua Li ^{a,b}, Pan Lu ^{a,b}, Zhenzhen Lu ^{a,b}, Jiayao Liu ^{a,b}, Chenhui Du ^c, Wei Wang ^{d,e}

^a School of Water and Environment, Chang'an University, Xi'an 710064, China

^b Key Laboratory of Subsurface Hydrology and Ecological Effects in Arid Region, Ministry of Education, Chang'an University, Xi'an 710064, China

^c School of Geological Engineering and Geomatics, Chang'an University, Xi'an 710064, Shaanxi, China

^d State Key Laboratory of Desert and Oasis Ecology, Xinjiang Institute of Ecology and Geography, Chinese Academy of Sciences, Urumqi 830011, China

^e Research Center for Ecology and Environment of Central Asia, Chinese Academy of Sciences, Urumqi 830011, China

ARTICLE INFO

ABSTRACT

Keywords:

Spatio-temporal variation
Driving factors
Geo-detector
Wavelet analysis

High-intensity human socioeconomic activities in Xi'an have caused fine particulate matter (PM_{2.5}) pollution. Understanding the spatial and temporal patterns and key factors influencing PM_{2.5} concentration was the basic step for taking targeted measures. Thus, spatial analysis techniques are used to reveal the temporal and spatial distribution characteristics of PM_{2.5} in Xi'an over a long time series; wavelet analysis and Geo-detector models are applied to assess the strength of the association between meteorological and socio-economic conditions on PM_{2.5} concentrations. The results illustrated that the average PM_{2.5} concentration was 40.13 µg/m³ in 2004 and peaked at 62.06 µg/m³ in 2011, before failing to 38.77 µg/m³ by 2018. The PM_{2.5} concentration distribution had a characteristic of high in winter and autumn but low in spring and summer, presenting a U-shaped profile. The main distribution of PM_{2.5} concentrations was oriented in a northeast-southwest direction, with obvious spatial autocorrelation and spatial aggregation characteristics. The resonance cycles of the meteorological and socio-economic elements and PM_{2.5} concentrations were synchronous and divergent at different scales. U-wind was the influencing factor on PM_{2.5} concentration with a positive correlation coefficient of 0.9. Before 2011, the interaction of temperature (Tem) and relative humidity (RH) had the greatest impact on PM_{2.5} concentrations. Additionally, the land use and cover change (LUCC) coupled with other factors had a large influence on PM_{2.5} concentrations. These relationships can shed new light on the underlying mechanisms of PM_{2.5} contamination at the city level, assisting relevant departments in developing effective PM_{2.5} pollution management strategies.

1. Introduction

Cities are the centers of human economic and productive activities (Yan et al., 2020). As cities in China are experiencing rapid urbanization and industrialization, their high energy consumption is accompanied by the deterioration of PM_{2.5} pollution (Yan et al., 2020). PM_{2.5} is becoming the primary pollutant of air pollution (Zhang et al., 2022). The burden of disease attributable to PM_{2.5} pollution is now estimated to be on a par with other major global health risks such as unhealthy diet and tobacco smoking, and PM_{2.5} pollution is now recognized as the single biggest environmental threat to human health.¹ Epidemiological researchers

also have confirmed that people exposed to PM_{2.5} are more likely to suffer from respiratory and cardiovascular disease and a shortened life expectancy (Lu et al., 2017b; Masiol et al., 2016). Hence, PM_{2.5} has attracted widespread attention from the government and society, while multidisciplinary scholars have been dedicated to PM_{2.5} pollution research (Liu et al., 2019; Mi et al., 2021; Ouyang et al., 2021; Shi et al., 2021). Moreover, the Chinese government introduced an *Air Pollution Prevention and Control Action Plan* in 2013,² demonstrating the determination of the Chinese government to combat air pollution and effectively reduce regional PM_{2.5} concentrations.

However, the wide geographical spread of China, with various

* Corresponding author at: School of Water and Environment, Chang'an University, Xi'an 710064, China.

E-mail address: dengsx@chd.edu.cn (S. Deng).

¹ The source of its website is <https://www.who.int/teams/environment-climate-change-and-health/air-quality-and-health>.

² The source of its website is https://www.gov.cn/zwgk/2013-09/12/content_2486773.htm.

regions exhibiting different meteorological and socioeconomic conditions and different PM_{2.5} distribution characteristics. For instance, Shijiazhuang and Hengshui have significantly higher PM_{2.5} concentrations than coastal cities such as Chengde and Qinhuangdao (Yan et al., 2018). Therefore, given the complexity of the influencing mechanisms of PM_{2.5} concentrations, strengthening the analysis of the impact mechanisms of PM_{2.5} pollution at city-level spatial and temporal scales is the premise and essential for the precise prevention and control of air pollution (Dong et al., 2022). Especially, Xi'an is the economic and cultural center of northwest China, and its unique topography, urbanization, and other energy structure issues have caused severe PM_{2.5} pollution. Though there are significant uncertainties, quantitatively researching these stochastic mechanisms and studying the relationships between these elements and concentrations of PM_{2.5} in Xi'an can provide insight into the patterns behind PM_{2.5} accumulation and dissipation. Overall, the accumulated literature on influencing factors can be broadly divided into two categories based on the research perspective: meteorological and socioeconomic factors.

Meteorological factors impact air quality in a variety of ways. Higher temperatures, for example, typically accelerate chemical reactions (Hogrefe, 2012). As a result, emissions from sources such as traffic or power plants will be transformed more quickly into pollutants such as ozone during global warming. Second, meteorological factors have an impact on PM_{2.5} transport and distribution by influencing both regional weather conditions and atmospheric circulation (Hogrefe, 2012). Furthermore, high relative humidity may contribute to haze formation (Li et al., 2019). Particles in the air are removed when precipitation reaches a certain level (Li et al., 2019). Thus, meteorological factors play an important role in the emission, formation, transportation, chemical transformation, and deposition of air pollutants. Studies have shown that a 1% increase in coal consumption increases PM_{2.5} emissions by 0.095% (Xu et al., 2016). As incomes and populations in coal-based cities increase, residents consume more energy, build more buildings, and buy more vehicles (Yan et al., 2021). This has led to a rapid increase in PM_{2.5} emissions. Moreover, a model of economic development driven by high investment and high pollution increases gross domestic product (GDP) and GDP per capita (GDPPC), but also at a huge environmental cost (Wu et al., 2021). It is thus evident that a scientific solution for haze control policies is necessary since complex meteorological and socio-economic factors cause haze pollution.

Cities in various stages of development present different meteorological conditions, energy consumption, income levels, and environmental regulations. Although scholars have examined PM_{2.5} pollution from eco-environmental, meteorological, and economic perspectives, many of them are based on macro-scale studies and few have investigated the mechanisms of PM_{2.5} formation and management at the city level supported by long time series data. From a practical point of view, we wondered what temporal and spatial changes have occurred to the PM_{2.5} concentrations over a long time series. What factors drive the changes in PM_{2.5} pollution at different periods? How to quantify the interactions between the drivers and how interpret the interactions at different stages? To this end, this study aims to investigate the spatio-temporal variations of PM_{2.5} concentrations in Xi'an using standard deviation ellipsoid analysis and spatial autocorrelation. Then, wavelet analysis and Geo-detector modeling are used to explore the relationship between PM_{2.5} and single or multiple driving factors at different scales over time. Our study supports environmental managers by providing a deeper understanding of the relationship between these drivers and urban pollution. This study also provides the information needed to formulate regional PM_{2.5} mitigation strategies.

The remainder of the paper is organized as follows: Part 2 presents the literature review. Part 3 presents the study domain, data, and methods. Part 4 shows the empirical results. Part 5 presents the discussions and implications of the paper. Part 6 concludes the paper.

2. Literature review

2.1. Research progress on the spatiotemporal distribution of PM_{2.5}

Based on sampling, chemical transport models and data from national control points, the researchers used statistical methods to reveal the patterns of regional particulate matter in Xi'an, Beijing, Wuhan, the Guan Zhong Plain (GZP), the Sichuan Basin (SCB), and the Bohai City Cluster (BCC) and the China region (Guang et al., 2019; Li et al., 2017; Li et al., 2015; Li et al., 2019; Lv et al., 2016; Niu et al., 2016; Song et al., 2016; Wang et al., 2014; Wang and Fang, 2016; Zhang et al., 2020a; Zhao et al., 2018; Zhao et al., 2019). Studies showed that annual mean PM_{2.5} concentrations in Xi'an, Beijing, and Wuhan were 250 µg/m³, 88.6 µg/m³, and 118.1 µg/m³. The maximum PM_{2.5} values in the southern GZP and SCB were 134.7 µg/m³ and 109.3 µg/m³, and PM_{2.5} concentrations in the BCC were higher in winter and autumn. Similarly, regional particulate matter in China is highest in winter and lowest in summer.

Furthermore, Spatial analysis techniques and Ordinary kriging interpolation were used to analyze the spatial variation characteristics of PM_{2.5} in major cities in China, Henan Province (HP), the Pearl River Delta (PRD), the middle of the Yellow River urban agglomeration (YR), and Xi'an (Mi et al., 2021; Xu et al., 2022; Yan et al., 2021; Zhao et al., 2020; Zhao et al., 2019). Studies found that most of the cities with higher PM_{2.5} pollution are located in eastern China, the spatial hotspot areas are mainly concentrated in northern HP, the cities in western PRD have higher PM_{2.5}, the urban agglomeration of PM_{2.5} in the middle reaches of the YR has obvious spatial clustering characteristics. In summary, most studies have been conducted based on the macro level and city-level studies have been documented but at short time scales.

2.2. Research progress on PM_{2.5} driving factors

Previous studies have investigated the various causes of PM_{2.5} from a natural science perspective using multivariate receptor models (Mi et al., 2021). However, studies have confirmed that the nature of PM_{2.5} exceedances lies in the social life of humans (Mi et al., 2021; Yan et al., 2021). Subsequently, researchers chose econometric methods to determine the socioeconomic factors influencing PM_{2.5}. Throughout the existing research, studies have used geographically weighted regression, correlation analysis, regression analysis, STIRPAT, and Logarithmic Mean Divisia Index to reveal the meteorological and socioeconomic factors of PM_{2.5} in Beijing, HP, Yangtze River Economic Zone, Green Valley, Canada and major cities in China (Csavina et al., 2014; Huang et al., 2020; Ji et al., 2018; Liu et al., 2019; Md. et al., 2016; Meng et al., 2019; Xu et al., 2022; Yan et al., 2021; Yan et al., 2020; Yang et al., 2018; Zhao et al., 2019). Studies indicated that wind speed has the most significant effect on PM_{2.5} concentrations in Beijing and Green Valley, land use type has the greatest effect on PM_{2.5} in HP, precipitation harms PM_{2.5} in the Yangtze River Economic Zone and the temperature has a positive effect on PM_{2.5} in low-income cities in China. For anthropogenic factors, the study found that population size, car ownership, and industrial structure were the main factors contributing to PM_{2.5} pollution in Chinese cities as well as industrialization rates contributing to PM_{2.5} in YR. However, regional natural factors had a greater impact on PM_{2.5} pollution than socioeconomic factors in China in 2015. Additionally, 37.2% of PM_{2.5} concentrations in Canada were strongly associated with traffic, industry-related emissions, and soil. These studies are helpful to detect the driving factors of PM_{2.5} on a large scale.

2.3. Research objectives

Although many studies have been reported on the spatial and temporal distribution of PM_{2.5} and the factors influencing it, and previous research has provided a wealth of findings, there are still three areas that require further study. First, previous studies have ignored the

uncertainty of interpolation methods to explore the spatial distribution of PM_{2.5}. The Chinese National Environmental Monitoring Center (CNEMC) started to establish a nationwide air quality monitoring network in China at the end of 2013 (Wang et al., 2020). The lack of long-term city-scale PM_{2.5} pollution data has limited our systematic understanding of the spatiotemporal variations of PM_{2.5} concentrations. Previous studies have analyzed the distribution of PM_{2.5} concentrations using spatial interpolation (Dong et al., 2022; Li et al., 2019; Zhang et al., 2020a; Zhang et al., 2022). Despite the monitoring systems across Xi'an, their coverage is not enough since it is often restricted to urban zones with more populated, leaving aside the rural areas. The application of spatial interpolation using relatively sparse monitoring systems may cause the spatial distribution of PM_{2.5} to have a 'bull's-eye' effect (higher values near the observation location), even if it is continuous. However, the development of PM_{2.5} concentration data based on remote sensing techniques and model fusion compensates for this shortcoming. Wang et al. (2020) utilized satellite-derived PM_{2.5} concentration data to analyze the spatial and temporal heterogeneity of PM_{2.5} in Xinjiang, demonstrating that remote sensing techniques can contribute to a more comprehensive understanding of the spatial variability of PM_{2.5}. Estimates of global PM_{2.5} concentrations were calculated by establishing advanced PM_{2.5} inversion algorithms based on multi-source remote sensing data and model simulations (van Donkelaar et al., 2016).

Second, few researchers, through investigation, have taken urban in China to research the spatiotemporal heterogeneity of PM_{2.5} and its driving factors on a long-term basis, especially from a socioeconomic perspective. Cities exhibit different characteristics of economic growth, energy consumption, industrial structure, population, and environmental context at different stages of development (Liu et al., 2019). Ignoring significant differences in the urbanization process may lead to biased or even misleading conclusions, and most previous studies have focused less on this difference in Xi'an. Xi'an, a megacity in western China, has been experiencing serious PM_{2.5} pollution due to its topography unfavorable to discharge and other energy structure issues. The rapid urbanization and industrialization of Xi'an from 2004 to 2018, during which time the urbanization rate grew to 74.01% in 2018, was the fastest stage of air quality deterioration.³ Therefore, a comprehensive and systematic study of the spatial and temporal variation of PM_{2.5} in Xi'an during long-term urbanization and the factors influencing it is needed, considering the urbanization process.

Third, previous studies have rarely examined the effects of city-level single or bivariate coupled factors on PM_{2.5} at different scales over time. Common methods used by scholars to study the spatial heterogeneity of PM_{2.5} concentration drivers include correlation analysis (Li et al., 2014; Li et al., 2019; Yan et al., 2018), geographically weighted regression (Mi et al., 2021; Ouyang et al., 2021; Zhao et al., 2020), and empirical model (Ji et al., 2018), etc. All of these methods have pros and cons. For example, correlation analysis methods are based on mathematical statistics of variables and may produce superimposed effects, making it hard to quantify the interactions between influencing factors and PM_{2.5} (Zhang et al., 2022). Given that the relationship between PM_{2.5} concentrations and influencing factors varies over time, we introduced Cross Wavelet Transform (XWT) and Wavelet coherence change (WTC) to capture the characteristics of this multi-scale variation to determine the relationship between the two variables based on the above research. Additionally, it has been shown that two meteorological factors contribute to or detract from pollutant concentrations and that one socioeconomic factor influences another socioeconomic factor while directly or indirectly affecting pollutant concentrations (Xu et al., 2016; Zhu et al., 2018). It still has some limitations if multicollinearity happens between different independent variables using the method described above. It becomes a great challenge to study the impact of

multiple influencing factors on PM_{2.5} at different time scales. We, therefore, focus on quantifying the effect of the interaction between meteorological factors on PM_{2.5} and the effect of socioeconomic factor interactions on PM_{2.5} based on Geo-Detector. Geo-Detector is a new statistical approach, that is commonly used to identify spatial differentiation and disclose the driving factors behind variables. It has the following advantages: ①The Geo-detector approach does not require any preconditions to be met, nor does it suffer from multicollinearity. ②It can detect the interaction of two factors on the dependent variable by using an interaction detector, to identify an interaction between two factors and the strength, direction, linearity, or nonlinearity of their interaction. Wavelet analysis and Geo-detector help us to understand the influence of single-factor or bivariate coupled factors on PM_{2.5} pollution in Xi'an. Thus, our findings are expected to provide more comprehensive and targeted perspectives for long-time series, city-level pollution mitigation. This scientific insight has undoubtedly expanded and enriched existing research.

3. Materials and methods

3.1. Study domain

Xi'an is the capital city of Shaanxi Province in western China. Xi'an is located in the middle of the Guanzhong Plain, with its topographic basin bounded by the Qinling Mountains to the south and the Loess Plateau to the north (Fig. 1). The unique geographical location, combined with emissions from anthropogenic sources including coal-burning, transport, and industry, leads to a higher level of pollutants in the atmosphere (Wang et al., 2014). Xi'an has a temperate semi-humid continental monsoon climate and annual precipitation is mainly concentrated in the summer and autumn seasons (Zhang et al., 2022). Up to 2018, Xi'an had a GDP of 8349.86 (100 billion yuan), a year-end permanent population of 1000.37 (10000 persons), and possession of civil vehicles of 325.63 (10000 units) vehicles, making it a megacity in China.⁴ However, with rapid urbanization and industrial development, the PM_{2.5} concentration in Xi'an increased faster. Therefore, this paper chooses Xi'an as the research area to reveal the spatiotemporal distribution pattern of PM_{2.5} and its driving factors.

3.2. Data resource

3.2.1. Data of annual average PM_{2.5} concentration

The global annual average surface-gridded datasets of PM_{2.5} concentrations with 0.01×0.01 degrees, which were evaluated by aerosol optical depth (AOD) retrievals from multiple satellite products, were provided by the Atmospheric Composition Analysis Group (van

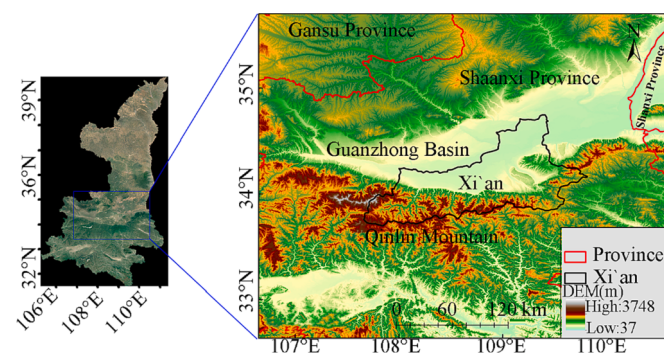


Fig. 1. The geographical location of Xi'an.

³ The source of its website is <https://tjj.xa.gov.cn/tjsj/tjgb/gmjhhshfzgb/60419917f8fd1c2073fa36d9.html>.

⁴ The source of its website is <https://tjj.xa.gov.cn/tjn/2019/zk/indexch.htm>.

Donkelaar et al., 2016) (<http://fizz.phys.dal.ca/~atmos/martin/>). These datasets integrate GEOS-Chem model simulation and ground measurement data. Numerous studies have been carried out at regional and national scales using these datasets (Huang et al., 2020; Lu et al., 2017a; Wang et al., 2020; Wu et al., 2021). Due to the spatial heterogeneity of PM_{2.5}, substantial research into the uncertainty of the satellite-derived values of PM_{2.5} has been done (Huang et al., 2020; Lu et al., 2017a; Wang et al., 2020). In this paper, hourly PM_{2.5} monitoring data were collected from 13 ground observation sites in Xi'an, provided by the China National Environmental Monitoring Centre (CNEMC), to fit gridded PM_{2.5} data from 2015 ~ 2018. A positive correlation was found between the annual average PM_{2.5} ground observation data and the corresponding PM_{2.5} gridded data with $R = 0.88$ (Supplementary materials, Figure S. 1). As a whole, the satellite-derived PM_{2.5} concentrations were reliable in this study area.

3.2.2. Data of meteorological factors

Previous work shows that the meteorological elements of temperature (Tem), Atmospheric pressure (P), U-wind (U), V-wind (V), Relative humidity (RH), and precipitation (Pre) impacted the spatial distribution of PM_{2.5} (He et al., 2018). Due to the inability to obtain continuous meteorological data, ERA5-Land monthly averaged data from 2004 ~ 2018 were used (<https://cds.climate.copernicus.eu/cdsapp#!/dataset/reanalysis-era5-land-monthly-means?tab=overview>). The meteorological factors (Tem, P, U, V) have a spatial resolution of $0.1 \times 0.1^\circ$. Additionally, ERA5 monthly averaged data provided the RH data with a spatial resolution of $0.25 \times 0.25^\circ$ (<https://cds.climate.copernicus.eu/cdsapp#!/dataset/reanalysis-era5-pressure-levels-monthly-means?tab=overview>). The continuity and integrity of the precipitation data was insured by using precipitation data from the Tropical Rainfall Measuring Mission satellite (TRMM) (<https://search.earthdata.nasa.gov/downloads/5396244909/collections/195655/links>). As a combined mission of the Japan Aerospace Exploration Agency (JAXA) and the National Aeronautics and Space Administration (NASA), the TRMM, was launched into space in 1997; it has shown excellent accuracy and applicability in most parts of the world. Hourly data from TRMM 3B43, which was reported at $0.25^\circ \times 0.25^\circ$, were used to monitor long-term precipitation from 2004 to 2018 in Xi'an.

3.2.3. Data of socioeconomic factors

This paper uses population density (PD) and population (POP), Gross Domestic Product (GDP), GDP per capita (GDPPC), industrial GDP (INGDP), and energy consumption per unit of GDP (EGDP) as socio-economic factors to measure the influence of human activities on the spatial distribution of PM_{2.5}, which provided by the Xi'an Statistical Yearbook (<http://tjj.xa.gov.cn/>). Additionally, the digital elevation model (DEM), Satellite Program's Operational Line-Scan System (DMSP-OLS), Suomi National Polar-orbiting Partnership Visible Infrared Imaging Radiometer Suite (NPP-VIIRS) (NSL), Normalized Difference Vegetation Index (NDVI), soil type (ST), and LUCC were also considered as socio-economic factors in this paper. See Supplementary materials, Text S. 1 provides a detailed presentation of socioeconomic data.

3.3. Methodology

3.3.1. Standard deviational ellipse analysis (SDE)

SDE was first introduced in 1926 by the sociologist Lefever as a geostatistical method for studying the spatial-spatial relationships of geographical elements (Lefever, 1926). Later, it was widely employed in many fields as a method for the descriptive exploration of geographic space (Ling et al., 2020). The area of the standard deviation ellipse represents the main area of the spatial distribution of the selected geographic features. The greater the difference between the values of the long and short semi-axes, the more pronounced the directionality of the data is indicated. The mean center is the center of all the data in two

dimensions and indicates the relative position of the geographical elements and their general evolutionary trajectory in different time series (Du et al., 2019). See Text S. 2 provides a detailed presentation of the SDE analysis.

3.3.2. Spatial autocorrelation statistics

Spatial autocorrelation analysis includes global spatial autocorrelation and local spatial autocorrelation. Based on Tobler's first law of geography, Patrick Moran invented the global Moran's I , which research has shown can be used to explore global spatial autocorrelation patterns of PM_{2.5} concentrations (Wang et al., 2020). Statistically, the Z_I -score can indicate significant clustering or dispersion of features. Thus, the Z_I -score is used to test the reliability of Moran's I (existence of spatial autocorrelation). The global Moran's I failed to identify differences in spatial autocorrelation between individual regions. Therefore, we introduced the Local Indicators of Spatial Association (LISA) to account for local nonstationary and location of hot spots. See Text S. 3 provides a detailed presentation of spatial autocorrelation statistics.

3.3.3. Wavelet analysis

Wave analysis is often used to obtain a complete representation of local and instantaneous phenomena that occur on different time scales, and to study the change characteristics of multiple time scales (Amantai et al., 2021). A detailed theory of it can be found in the reference Hudgins and Huang (1996). This method is widely used in geophysics, meteorology, hydrology, astronomy, environmental science, and other disciplines (Amantai et al., 2021; Hu et al., 2017; Li et al., 2014). See Text S. 4 provides a detailed presentation of wavelet analysis.

3.3.3.1. Cross Wavelet Transform. Cross Wavelet Transform (XWT) is developed from traditional wavelet analysis and is often used to comprehensively test the relationship between two time series. The XWT is characterized by strong signal coupling and resolution capabilities. The resonance period and phase relationship with higher resonance energy in the 2-period series can be easily analyzed (Amantai et al., 2021). When 2-period series $x(t)$ and $y(t)$ are given, the cross wavelet transforms formula can be defined as:

$$Z_{xy} = Z_x Z_y^* \quad (1)$$

where Z_x and Z_y^* represents the continuous wavelet of $x(t)$ and $y(t)$ respectively. $*$ represents a complex conjugate.

3.3.3.2. Wavelet coherent. Wavelet coherence (WTC) relies on the search frequency band and the time interval between two processes to identify their possible relationship, and the wavelet coherence change can characterize the consistency of the cross wavelet transform in the time-frequency space (Amantai et al., 2021). The significant correlation between the low-energy regions of the two-time series is analyzed by cross-wavelet aggregation. This process compensates for the shortcomings of the wavelet energy spectrum in identifying low-energy regions instead of high-energy regions (Hu et al., 2017). The degree of local correlation between two time series $x(t)$ and $y(t)$ is measured by wavelet coherence and defines the complex wavelet coherence P_{xy} .

$$P_{xy} = S(Z_{xy}) / \sqrt{[S(|Z_x|^2)S(|Z_y|^2)]} \quad (2)$$

where S is the smooth spectrum operation in the time-frequency domain.

3.3.4. Geo-Detectors

Geo-detector is a statistical method for detecting the spatial heterogeneity of influences and revealing the driving forces behind them (Wang and Xu, 2017). Geo-Detector to detect interaction relationships between factors was widely used in an Ecological environment (Jing

et al., 2020), agriculture (Chu et al., 2020), and public health (Zhang et al., 2020b). We used the interaction detector and the ecological detector to explore the interplay of various factors (RH, V, U, Pre, Tem, P, NSL, PD, POP, NDVI, ST, LUCC, DEM, GDPPC, INGDP, EGDP, GDP) to the dependent variable ($PM_{2.5}$) and detect the significance of different effect variables on the dependent variable, respectively. See Text S. 5 provides a detailed presentation of Geo-Detector.

3.3.5. Evaluation criterion

December, January, and February are recorded as winter, correspondingly March to May are spring, June to August is summer, and September to November is autumn.

3.3.6. The flowchart of This study

Based on the objective of this study, this manuscript is organized as presented in the flowchart of the methodology (Fig. 2). First, the temporal and spatial characteristics of annual $PM_{2.5}$ concentrations were explored by SDE analysis and spatial autocorrelation statistics. wavelet analysis tools were used to clarify the cyclical variation between $PM_{2.5}$ and drivers and the influence of single factors. Finally, based on the use of the Geo-Detector combined with multisource data, the bivariate coupling relationship between $PM_{2.5}$ and the drivers was examined.

4. Results

4.1. Spatiotemporal variation pattern of $PM_{2.5}$

4.1.1. Spatiotemporal pattern of $PM_{2.5}$ concentrations

The temporal distribution of $PM_{2.5}$ annual average concentrations in Xi'an from 2004 to 2018 is presented in Fig. 3. The annual average $PM_{2.5}$ concentrations showed a trend upward initially and then downward (Fig. 3). The average value of the $PM_{2.5}$ concentration in Xi'an was $40.13 \mu\text{g}/\text{m}^3$ in 2004 and reached a maximum value of $62.06 \mu\text{g}/\text{m}^3$ in

2011, an increased rate of 54.64%. From 2011 to 2015, during the implementation of the 12th Five-Year Plan, the Chinese government set corresponding emission reduction targets to combat air pollution. The $PM_{2.5}$ concentrations, thus have shown a gradual downward trend. Moreover, The $PM_{2.5}$ concentration fell to $38.77 \mu\text{g}/\text{m}^3$ by 2018, a drop of 37.52% compared to 2011. As a whole, the air quality in Xi'an has continuously improved.

The spatial variation of $PM_{2.5}$ concentrations in Xi'an from 2004 to 2014 was presented in Figure S. 2. The results showed that the distribution of $PM_{2.5}$ concentrations was significantly higher in the northern regions than in the eastern, southern, and western regions, with an average maximum $PM_{2.5}$ concentration of $100.3 \mu\text{g}/\text{m}^3$ and clear urban characteristics. There was also a trend of increasing and then decreasing $PM_{2.5}$ concentrations in Xi'an. From 2004 to 2011, $PM_{2.5}$ concentrations increased from a maximum mean concentration of $74.3 \mu\text{g}/\text{m}^3$ to $100.3 \mu\text{g}/\text{m}^3$, an increase of 34.99%. Between 2011 and 2014, there was a clear downward trend in $PM_{2.5}$ concentrations.

Monthly, seasonal, and annual average $PM_{2.5}$ ground-based observations were calculated for 13 monitoring stations (Fig. 4). The spatial distribution of the highest and lowest $PM_{2.5}$ concentrations in Xi'an from 2015~2018 is reflected in Fig. 4 (a1,b1,c1, and d1). The box plot of monthly variations in $PM_{2.5}$ concentration in Xi'an from 2016 to 2018 is reflected in Fig. 4 (A, B, C, D). Overall, from 2015 to 2018, the inter-month variation in $PM_{2.5}$ concentrations follows a U-shaped pattern, with a decreasing tendency from January to July, and an upward trend from August to December. However, from January to June 2015, the monthly average concentration of $PM_{2.5}$ dropped from $94.02 \mu\text{g}/\text{m}^3$ to $34.0 \mu\text{g}/\text{m}^3$; there has been an upward trend since July. From July to December, the monthly average concentration of $PM_{2.5}$ increased from $41.17 \mu\text{g}/\text{m}^3$ to $108.00 \mu\text{g}/\text{m}^3$. The monthly average concentration of $PM_{2.5}$ from January to July 2016, declined from $111.14 \mu\text{g}/\text{m}^3$ to $25.23 \mu\text{g}/\text{m}^3$, a decrease of 77.30%. Monthly average $PM_{2.5}$ concentrations fluctuated the greatest in December, followed by November. $PM_{2.5}$

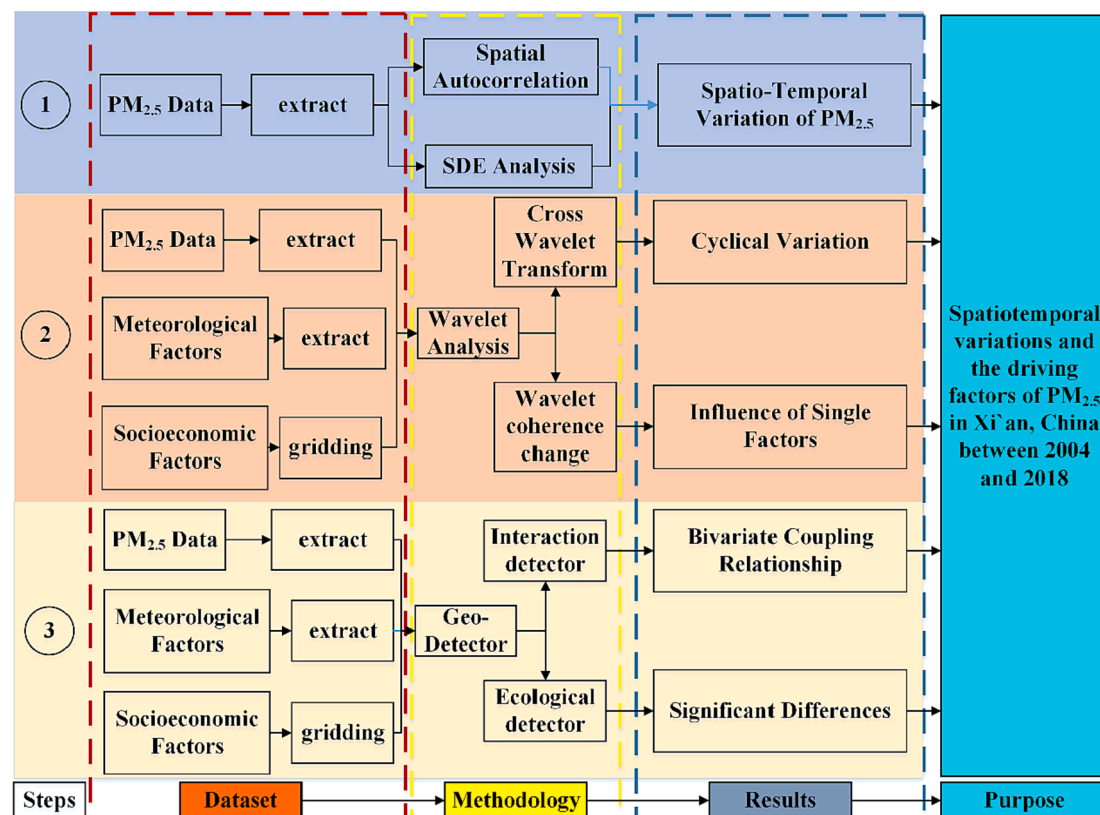


Fig. 2. The flowchart of the methodology.

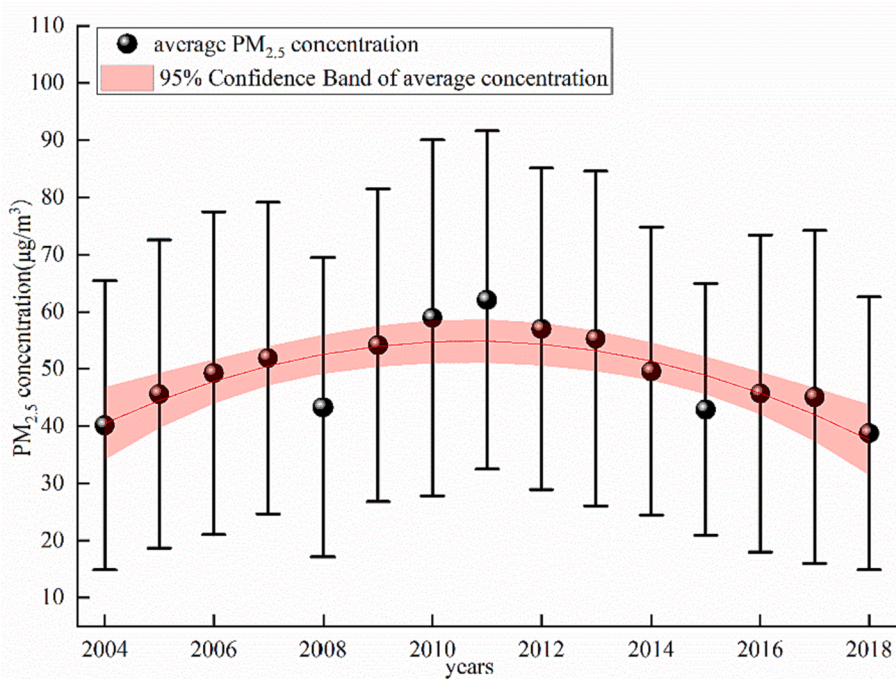


Fig. 3. Annual trends in PM_{2.5} concentrations from gridded data for 2004 ~ 2018.

concentration exhibited a clear seasonal variation, with winter > autumn > spring > summer generally (Fig. 4E). Specifically, in 2015, the average PM_{2.5} concentration was 68.55 μg/m³ in winter, 56.83 μg/m³ in autumn, and 46.85 μg/m³ in summer. In 2016, the average PM_{2.5} concentration was 93.55 μg/m³ in winter, 55.54 μg/m³ in autumn, and 40.48 μg/m³ in summer. In Xi'an, the annual PM_{2.5} concentrations slightly decreased over 2015 ~ 2018 (Fig. 4F).

Fig. 5 provides a map of the directional distribution of PM_{2.5} concentrations in Xi'an based on SDE analysis. The result shows that the main distribution of PM_{2.5} concentrations was aligned in the northeast-southwest direction. The median center was clear but gradually moves from northeast to southwest from 2004~2015; however, from 2015 to 2018, it gradually moved to the northeast slowly. Moreover, the surface area of the ellipse showed a trend of first increasing and then decreasing during the study period. The spatial distribution of the PM_{2.5} concentration gradually became concentrated after 2008.

In summary, the spatial variation in the annual average PM_{2.5} was significant, showing a trend of high in the north and low in the south. The seasonal and monthly variations in PM_{2.5} were obvious, mainly showing high concentrations in winter and low concentrations in summer, and high PM_{2.5} concentrations in January and low in July. The main distribution direction of PM_{2.5} concentrations was northeast-southwest.

4.1.2. Spatial agglomeration characteristics of PM_{2.5} concentration

A global Moran's I scatter plot of PM_{2.5} concentrations is shown in Fig. 6. The horizontal axis in the scatter plot represents the standardized PM_{2.5} concentration, while the vertical axis represents the neighboring PM_{2.5} concentration values calculated from the Euclidean distance-based spatial weight matrix, also referred to as the lagged PM_{2.5} concentration. It can be seen that the value of Moran's I is in the range of 0.979~0.985 with a declining trend. All values of Moran's I were significant ($p \leq 0.01$) within the study period. The majority of dots are clustered in the first and third quadrants, which means that most areas display a positive spatial autocorrelation of PM_{2.5} concentrations. The high-high cluster and low-low cluster in the LISA graph can explain this phenomenon (Figure S. 3). From the results of local spatial autocorrelation findings, high-high clusters are defined as high-concentration

areas of PM_{2.5}; low-low clusters are defined as the low PM_{2.5} concentration areas. Hotspots mainly occurred in the north, northeast, and northwest of Xi'an. The cold spots (low-low clusters) of pollution are mainly located in the southwest, south, and parts of the east of Xi'an. Overall, PM_{2.5} shows a clear spatial autocorrelation and a clear differentiation between cold and hot spots.

4.2. Delay correlation analysis of PM_{2.5} and driving factors

4.2.1. Delay correlation analysis of PM_{2.5} and meteorological factors

We apply XWT and WTC to explore the influencing factors of PM_{2.5} and other meteorological elements in Xi'an. See Text S. 4 provides a detailed description. As shown in Fig. 7, PM_{2.5} and annual average RH had 6 significant resonance periods in the high-energy region (Fig. 7a) and 16 significant resonance periods in the low-energy region (Fig. 7A). The phase angle of the two high-energy (Fig. 7a) and low-energy (Fig. 7A) regions was $90 \pm 45^\circ$, which indicates that RH changes ahead of PM_{2.5}. During the short period from 2004 to 2018, the RH was positively correlated with PM_{2.5}, with a correlation coefficient of approximately 0.85. In 2004~2006 (50~140n), the phase angle was close to 90° , which indicated that the V wind was ahead the PM_{2.5} in this resonance period with a correlation coefficient of approximately 0.8 (Fig. 7B). A downward vertical phase angle appeared in the high-energy region (2014~2016), illustrating that the U wind lagged behind the change in PM_{2.5} during this resonance period. The low-energy region (Fig. 7C) presented an extremely pronounced positive correlation with a correlation coefficient of up to 0.9, which meant that U wind was the dominant factor of PM_{2.5} variability. There was a clear negative correlation between Pre and PM_{2.5}, with a correlation coefficient of approximately 0.8 (Fig. 7D). From 2004 to 2018, the phase angle of the low energy region mainly showed a horizontal tendency to the right (Fig. 7E), which indicated that Tem was positively correlated with PM_{2.5} with a correlation coefficient of 0.8.

4.2.2. Delayed correlation analysis of PM_{2.5} and socioeconomic parts

The correlation coefficient between NSL and PM_{2.5} varied from cycle to cycle. (Fig. 8a). The resonant period of the high-energy region of PD was considerably higher than that of NSL. (Figure S. 4a, b). In the low-

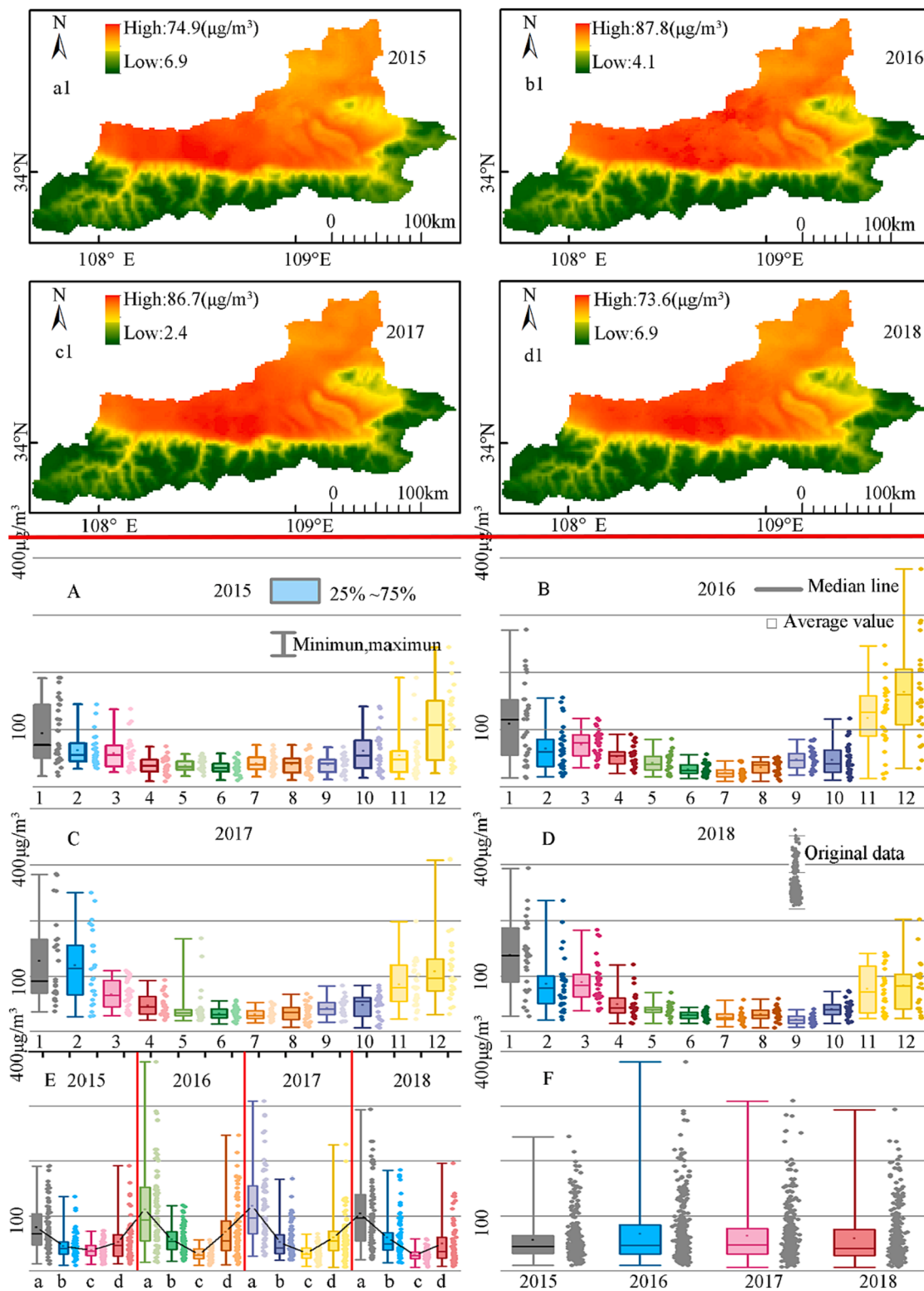


Fig. 4. Temporal variation in PM_{2.5} in Xi'an during 2015–2018 (above the red line are the satellite-based raster data, and the following are the ground monitoring site data: the numbers 1~12 represent January to December; a, b, c, and d represent winter, spring, summer, and autumn respectively). (For interpretation of the references to colour in this figure legend, the reader is referred to the web version of this article.)

energy region (Fig. 8c), the phase angles of the two were consistent with the right, showing an extremely significant positive correlation (0.85). A vertical downward phase angle appeared during the long period (2006~2014), indicating that the NDVI lagged behind the variation in PM_{2.5} over this resonance period (Figure S. 4d). The phase angle of both

showed a smoothing trend on the left, with large negative correlation, the correlation coefficient was as high as 0.8. (Fig. 8d). From 2013 to 2015, the phase angle in the high cycle of the high energy region was close to the vertically upward direction, indicating that the change in PM_{2.5} was 90° ahead of the LUCC phase (Figure S. 4f). From 2014 to

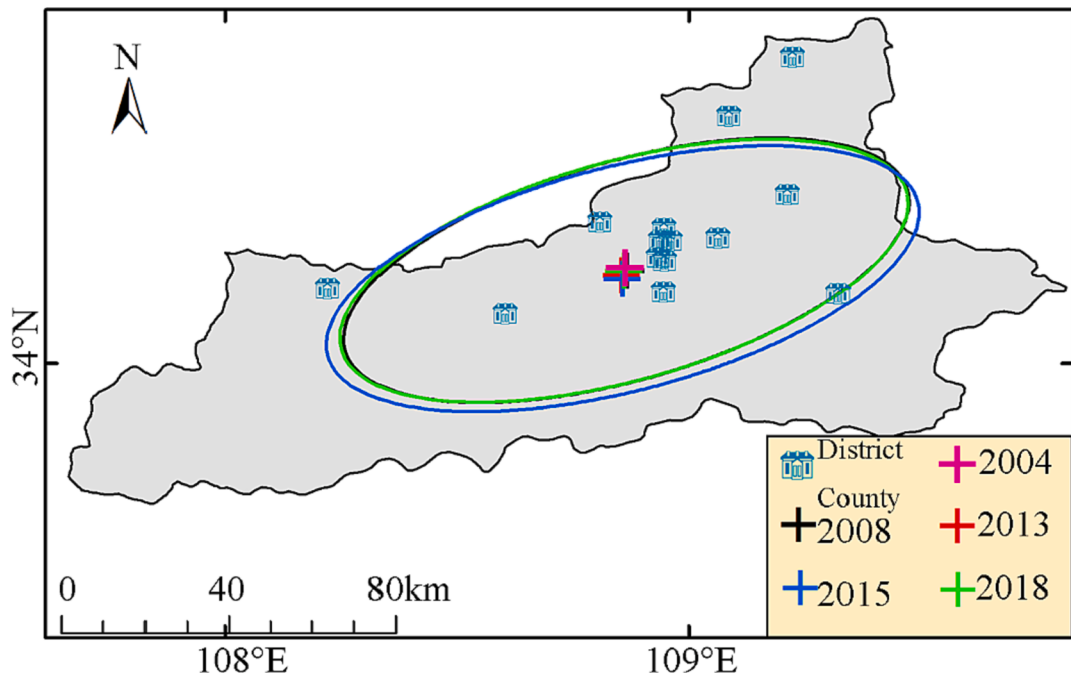


Fig. 5. Spatial changes in the median center and standard deviation ellipses of $\text{PM}_{2.5}$ concentrations.

2018, LUCC and $\text{PM}_{2.5}$ changed in the same phase of the high cycle, and the correlation coefficient was 0.85 (Fig. 8f). There was an inverse phase change in the high period of the low energy region, and the correlation coefficient was -0.65 (Fig. 8g). A phase angle of 90° was found in the high-energy region in the high cycle from 2014 to 2016 (Figure S. 4 h). The phase angles of both were right, demonstrating a negative correlation with a correlation coefficient of 0.7 (Fig. 8h). INGDP was shown to positively affect $\text{PM}_{2.5}$ concentrations (Fig. 8i). Moreover, EGDP and $\text{PM}_{2.5}$ showed a positive correlation coefficient of 0.75 (Fig. 8j). Interestingly, the less resonant cycles of EGDP after 2011 indicated a reduction in the contribution to $\text{PM}_{2.5}$. INGDP was shown to positively affect $\text{PM}_{2.5}$ concentrations (Fig. 8i). Another important finding was that the impact of GDP on $\text{PM}_{2.5}$ was positively correlated (2004~2011) and negatively correlated (2012~2018) (Fig. 8k).

The results above indicated that $\text{PM}_{2.5}$ was influenced by various weather and socioeconomic factors. Indeed, the existence of resonance cycles of meteorological or socioeconomic factors in different periods indicated that $\text{PM}_{2.5}$ pollution was influenced by the coupled effects of multiple meteorological or socioeconomic factors, exemplifying the rationale for further exploring the effects of multiple coupled factors on $\text{PM}_{2.5}$ over different periods.

4.3. Analysis of driving factors of $\text{PM}_{2.5}$ pollution in Xi'an

4.3.1. The potential interaction effects of meteorological driving factors on $\text{PM}_{2.5}$ in Xi'an

By comparing the comprehensive contribution of two factors to $\text{PM}_{2.5}$ and their respective effects, the interaction of any two factors (symbolized by \cap) was analyzed. A total of 15 kinds of various interactions among the 6 factors were computed each year with the interaction detector (Fig. 9). The results showed that $C(\text{Tem} \cap \text{Pre}) = 0.967$, and $C(\text{Tem} \cap \text{RH}) = 0.965$ were ranked first to second between the interactions of meteorological factors and $\text{PM}_{2.5}$ in 2004, respectively (Fig. 9). In 2006, $C(\text{Tem} \cap \text{RH}) = 0.957$, $C(\text{P} \cap \text{RH}) = 0.957$, and $C(\text{Tem} \cap \text{Pre}) = 0.942$ had the strongest explanatory power for $\text{PM}_{2.5}$ (Fig. 9). Interestingly, the impact on $\text{PM}_{2.5}$ was observed to have an identical stronger explanatory power of $\text{Pre} \cap \text{RH}$ and $\text{Tem} \cap \text{U}$ in 2011 (Fig. 9). In 2015, it became Tem and RH , P and RH with C values of 0.971 and 0.969, respectively (Fig. 9). $C(\text{Pre} \cap \text{RH}) = 0.964$, and $C(\text{V} \cap$

$\text{P}) = 0.963$ were ranked first to second between the interactions of meteorological factors and $\text{PM}_{2.5}$ in 2018 (Fig. 9).

The ecological detector was examined to understand the significance of varying influence among the 6 factors (Figure S. 5). What is interesting about the data in Fig. 9 is that the impact of all meteorological factors on $\text{PM}_{2.5}$ is a bivariate boost. The results also showed that three quarters were statistically significant (Figure S. 5). In contrast, there was no statistical significance between RH and V wind from 2004 to 2017 (Figure S. 5).

4.3.2. The potential interaction effects of socioeconomic driving factors on $\text{PM}_{2.5}$ in Xi'an

A total of 66 kinds of various interactions among the 11 factors were computed each year (Figure S. 6). The results showed that $C(\text{INGDP} \cap \text{LUCC}) = 0.988$ and $C(\text{GDP} \cap \text{LUCC}) = 0.985$ were ranked first to second in 2004, respectively. Correspondingly, $C(\text{EGDP} \cap \text{ST}) = 0.969$, and $C(\text{EGDP} \cap \text{GDPPC}) = 0.968$ ranked first and second in 2005; however, in 2006, $C(\text{DEM} \cap \text{GDPPC}) = 0.967$ and $C(\text{EGDP} \cap \text{ST}) = 0.965$ had the strongest explanatory power for $\text{PM}_{2.5}$.

Interestingly, the impact on $\text{PM}_{2.5}$ had an identical stronger explanatory power of $\text{LUCC} \cap \text{NDVI}$ and $\text{LUCC} \cap \text{DEM}$ with a C value of 0.982 in 2013; the same phenomenon occurred in 2016. The impact on $\text{PM}_{2.5}$ had an identical stronger explanatory power of $\text{LUCC} \cap \text{NDVI}$ and $\text{LUCC} \cap \text{EGDP}$ had C values of 0.973 in 2016. The GDPPC and INGDP , NDVI , and INGDP with a C value of 0.970 and 0.968 in 2016, respectively. $C(\text{DEM} \cap \text{ST}) = 0.966$ and $C(\text{GDPPC} \cap \text{EGDP}) = 0.964$ were ranked first and second between the interactions of meteorological factors and $\text{PM}_{2.5}$ in 2018. Since 2013, the coupling effect of NSL and other socioeconomic factors on $\text{PM}_{2.5}$ has not entered the top 10%; the same phenomenon occurs in the coupling of PD and POP and other socioeconomic factors. Additionally, compared with other socioeconomic factors, the C value of the effect of the coupling of NSL , PD , and POP on $\text{PM}_{2.5}$ has been relatively low.

The ecological detector was examined to understand the significance of varying influence among the 11 factors (Figure S. 7). What is interesting about the data in Figure S. 7 is that the impact of over 90% of meteorological factors on $\text{PM}_{2.5}$ is a bivariate boost; nevertheless, in 2013~2014, the coupling effect of NSL and other socioeconomic factors was univariate weakened. Three-quarters of the data were statistically

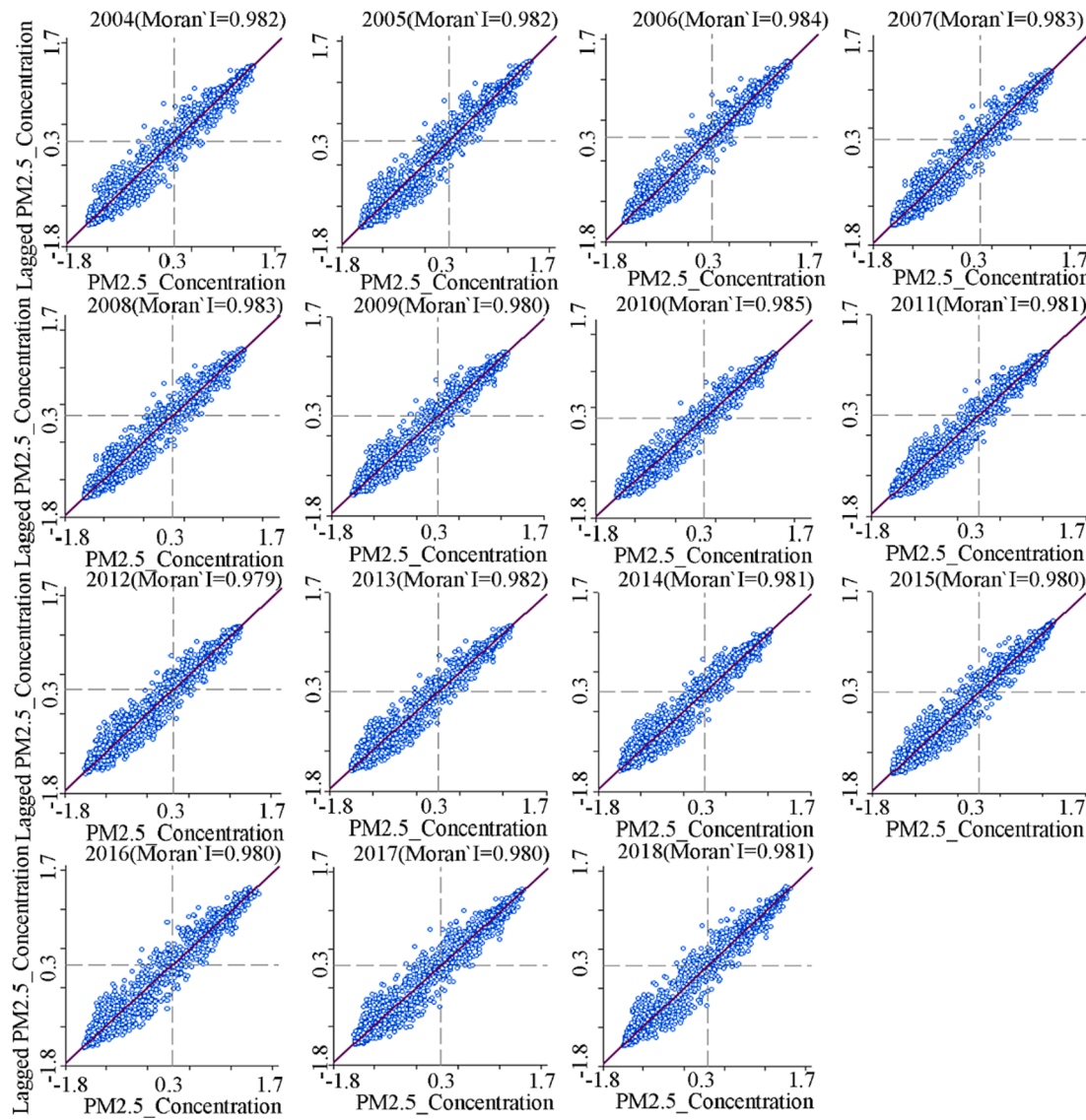


Fig. 6. Global Moran's I scatter plots of $\text{PM}_{2.5}$ concentrations (2004 ~ 2018).

significant.

In general, the effect of influencing factor interactions on $\text{PM}_{2.5}$ concentrations varied between periods. In terms of meteorological factors, Tem and RH had a strong influence on $\text{PM}_{2.5}$ concentrations before 2011, followed by Tem and Pre, and Pre and RH dominated after 2011. In terms of meteorological factors, the coupling of LUCC with other factors had a greater impact on $\text{PM}_{2.5}$ concentrations. The bivariate coupling of PD and POP factors had a smaller effect on $\text{PM}_{2.5}$ than the other factors.

5. Discussion

To clarify the evolution of $\text{PM}_{2.5}$, we revealed the long-term evolution of $\text{PM}_{2.5}$ with the help of SDE and geostatistical methods. To further explore the cyclical variations and determinants of $\text{PM}_{2.5}$ concentrations, we used wavelet analysis and Geo-Detector approaches to quantify the resonance period and interannual change of driving forces. Our results reveal trends in long-term $\text{PM}_{2.5}$ concentrations and the varying intensity of meteorological and socioeconomic factors influencing $\text{PM}_{2.5}$ concentrations over time. Our study is a valuable complement to the long-time series $\text{PM}_{2.5}$ monitoring problem and provides the necessary reference basis for the prevention and control of air pollution in Xi'an.

5.1. Analysis of the temporal and spatial evolution of $\text{PM}_{2.5}$

The first finding is the significant spatial and temporal variability and spatial autocorrelation of the $\text{PM}_{2.5}$ long-time series. Specifically, our study indicates that annual $\text{PM}_{2.5}$ shows an inverted V trend, which demonstrates the effectiveness of anthropogenic treatment. Energy-saving and emission reduction behaviors such as closing down factories and restricting car numbers have reduced emissions of particulate matter, SO_2 , and nitrogen oxides, decreasing the concentrations of $\text{PM}_{2.5}$ (Xu et al., 2022). This result was also reported by Duan et al. (2022). We also revealed that the seasonal divergence of $\text{PM}_{2.5}$ concentrations in Xi'an is evident, with low levels in summer and high levels in winter. This result of the $\text{PM}_{2.5}$ seasonal distribution is consistent with that of Wang and Fang. (2016) who found it in Beijing and Tianjin. However, contrary to this paper, the ratio of winter to summer $\text{PM}_{2.5}$ concentrations in the tropical cities of Lijiang and Aba is close to 1, resulting from less meteorological variability (Li et al., 2019). Conversely, local wildfires cause the highest $\text{PM}_{2.5}$ concentrations in Cali during the summer (Casallas et al., 2022). There are several reasons for our result. First, the government heats homes and offices in Xi'an in the winter by burning coal. This heating method produces large amounts of respirable particulate matter, especially $\text{PM}_{2.5}$. Second, the accumulation of atmospheric

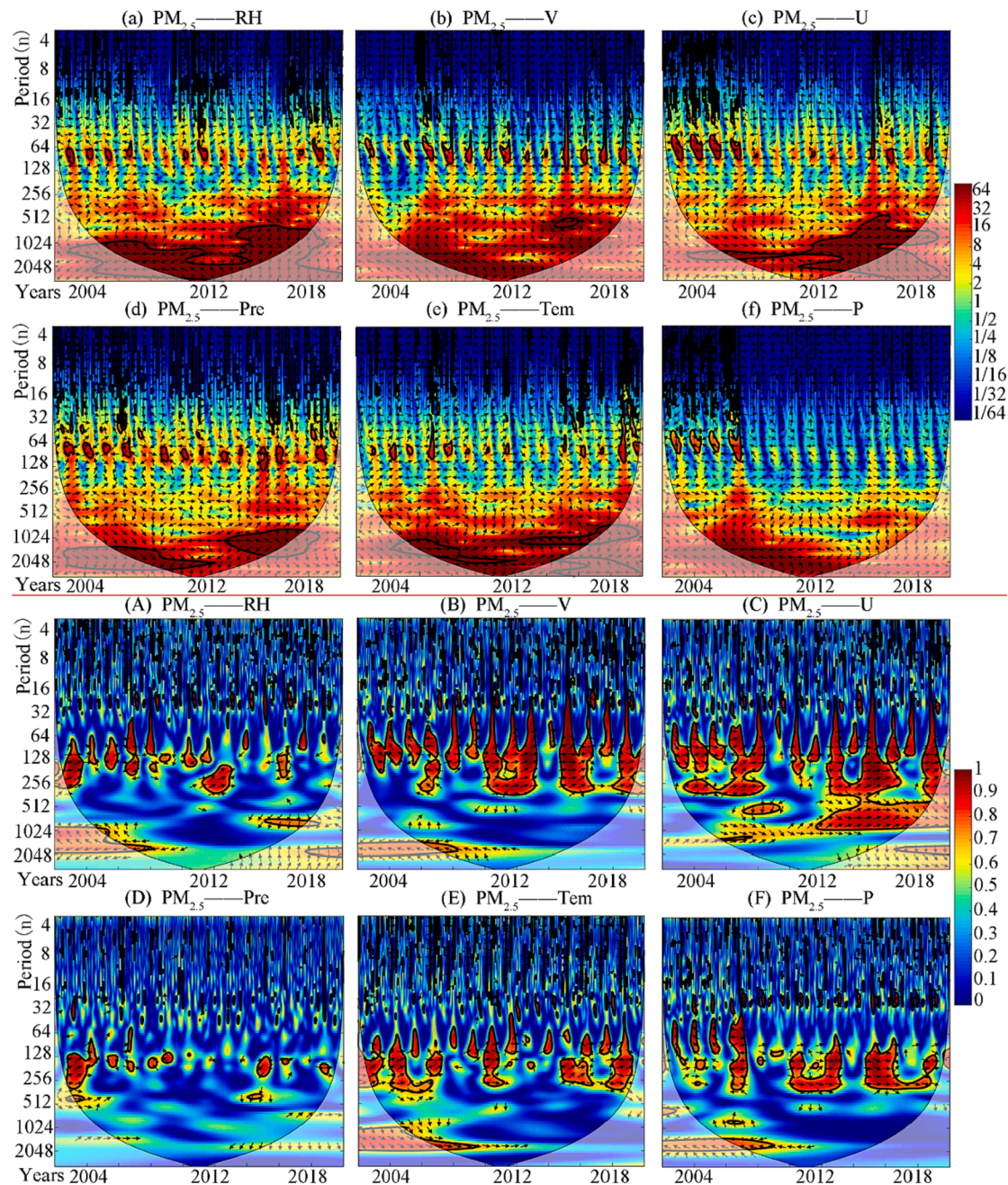


Fig. 7. Cross wavelet power spectrum (a ~ f, above the red line) and cross wavelet coherence spectrum (A ~ F, below the red line) between $\text{PM}_{2.5}$ and meteorological aspects. (For interpretation of the references to colour in this figure legend, the reader is referred to the web version of this article.)

pollutants is attributed to meteorological conditions in the north that are unfavorable (winter stagnant weather and inversions) for the dispersion of pollutants (Liu et al., 2015). Another study showed that regional transport aggravated $\text{PM}_{2.5}$ concentrations in Beijing during winter (Sun et al., 2022). Open-pit mining has been found as being responsible for high concentrations of $\text{PM}_{2.5}$ in Northern Colombia during winter (Rodríguez-Gómez et al., 2021). Third, dust storms are frequent in northwest China in late winter and early spring; this is when long-range transport of soil and desert-derived mineral dust caused by wind erosion affects the quality of the study area's atmosphere (Song et al., 2016). This also explains the elevated $\text{PM}_{2.5}$ concentrations in spring. Similarly, the cities located near the Taklamakan Desert (Kashgar, Hotan) have high $\text{PM}_{2.5}$ concentrations in spring caused by sandstorms (Rupakheti et al., 2021). High $\text{PM}_{2.5}$ concentrations occur in autumn due to increased open biomass burning (Wang et al., 2017). Studies also

attributed biomass burnings to causing poor-quality episodes in the Villavicencio and Cauca River Valley region, owing to the production of sugarcane and derivatives, which is one of their main economic activities (Mateus-Fontecha et al., 2022; Rodríguez-Gómez et al., 2021). In the Yangtze River Delta (YRD) urban megaregion, however, the burning of rice straw in earlier summer increases the $\text{PM}_{2.5}$ concentration (Zhao et al., 2019).

Areas with low LISA concentrations coincide with high mountainous areas where dense forests lead to strong absorption of $\text{PM}_{2.5}$. The number of grid units contained in the cold spot is different from that of the hot spot in the time series and basically remains stable. The northern, northeastern, and northwestern areas of Xi'an are the main locations of hotspot concentrations. This phenomenon is influenced by the terrain and regional transportation. This result is similar to that of Londoño Pineda and Cano. (2021) found topography affects $\text{PM}_{2.5}$

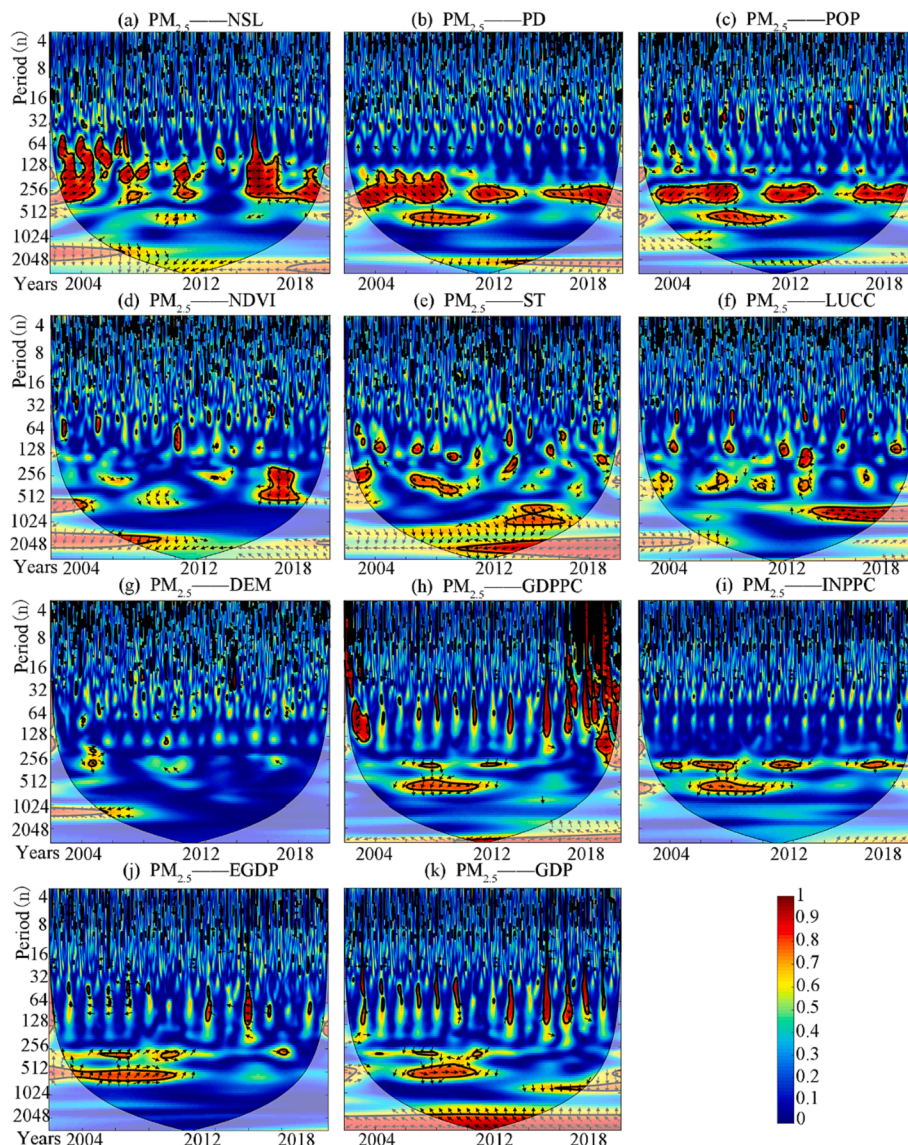


Fig. 8. Cross wavelet coherence spectrum between PM_{2.5} and socioeconomic factors (a ~ k).

concentration in Aburrá Valley. There is no high-low or low-high local spatial autocorrelation type of grid, indicating that the annual average concentration of PM_{2.5} showed extremely strong local spatial autocorrelation characteristics.

5.2. Individual and synergistic effects of different meteorological factors on PM_{2.5}

The second finding was that RH, U, V, and Tem had a positive contribution to PM_{2.5} while Pre had the opposite. This can be explained by a high level of RH contributing to moisture being easily absorbed and expanded by the soluble particles in PM_{2.5}; eventually, considerable PM_{2.5} accumulates in the atmosphere. In this study, the impact of wind direction was positive in the model evaluation results. This may be due to the diffusion effect of atmospheric pollutants in upwind cities and the case with which pollutant concentrations in downwind cities increases (Huang et al., 2020). Compared to other meteorological factors U-winds have a longer covariation period in the high and low-energy regions. This highlights the fact that U-winds have the greatest impact on PM_{2.5}. There was a clear negative correlation between Pre and PM_{2.5}. Reports have shown that Pre can directly eliminate air pollutants, resulting in a rapid decline in PM_{2.5} concentration (Huang et al., 2020; Zhang et al.,

2020a). The result of Tem may be explained by the fact that high Tem generally has a higher boundary layer, which is conducive to the convection and diffusion of pollutants; low Tem easily forms stable weather, which is conducive to the accumulation of PM_{2.5} (Xu et al., 2014). Another possible explanation for that higher Tem is conducive to photochemical reactions, and is conducive to the conversion of gaseous pollutants to PM_{2.5}, causing the concentration of PM_{2.5} to rise (Huang et al., 2020). Similar characteristics have been observed in other cities and regions, such as Urumqi, Lanzhou, and Sichuan Basin (Rupakheti et al., 2021; Zhao et al., 2018).

The third finding was that, prior to the 2010 turning point, the coupling effect of Tem and RH mainly affected PM_{2.5}; after 2010, the double coupling effect of Pre, RH, and V wind dominated. A possibility is that increasingly higher Tem and lower RH triggered the decrease in soil moisture, which adversely affected surface vegetation and significantly benefited dust emission and transportation. A higher frequency of Pre means a higher level of RH in the air; their interactions help eliminate PM_{2.5}. The coupling effect of V wind with other meteorological factors was relatively weak. All interactions were detected as two-factor enhancement, indicating that the combined effect of multiple factors significantly enhanced the explanatory power of PM_{2.5} concentration changes, and their influence on PM_{2.5} concentration changes was

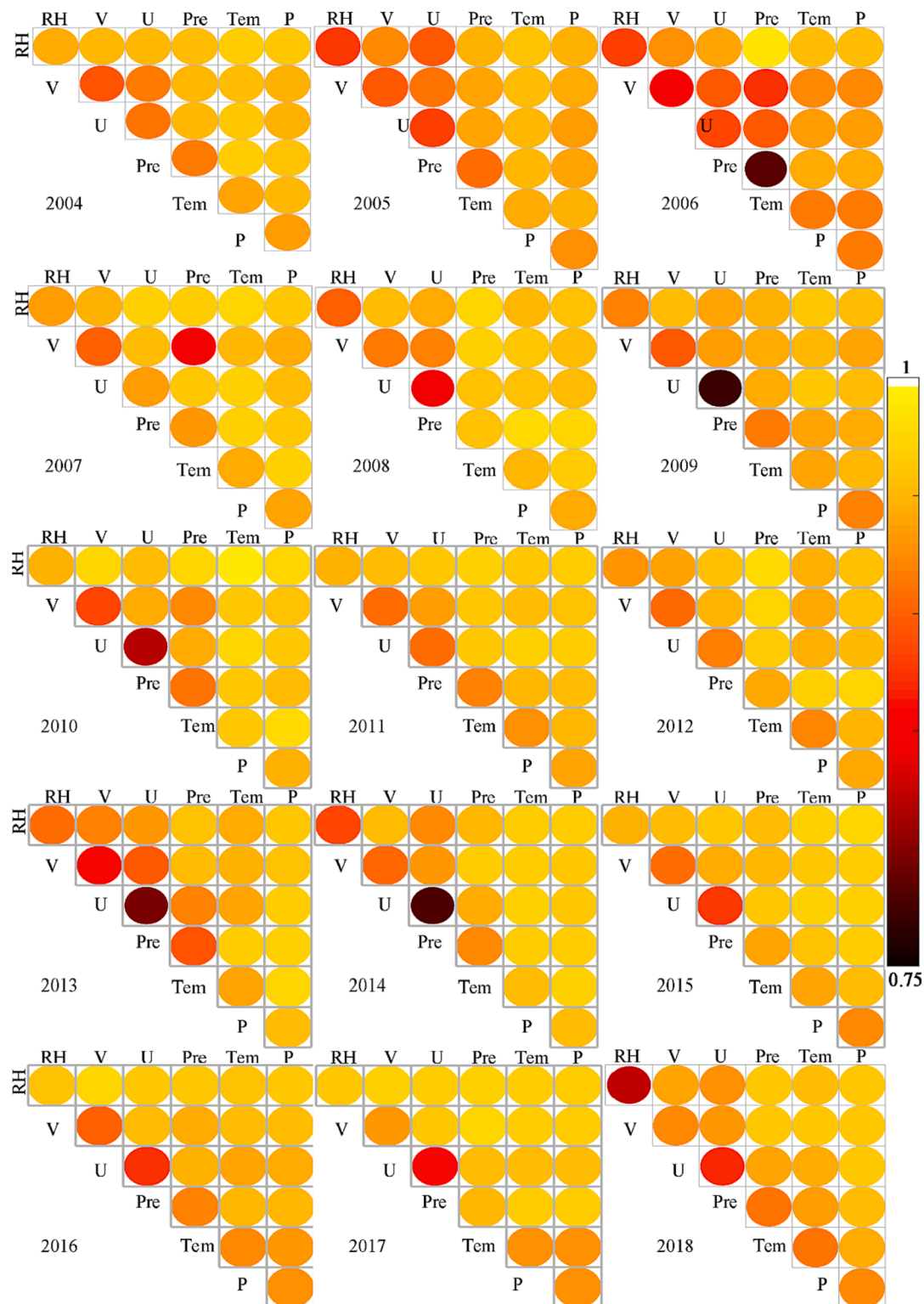


Fig. 9. The interaction detector C value of meteorological controlling factors.

therefore more significant. Wavelet analysis showed that there were different scaled resonance periods as well as time lag periods and different degrees of correlation between PM_{2.5} and various meteorological factors or socioeconomic factors. We also determined that there was synchrony between the resonance cycles of PM_{2.5} and the influencing factors; this further suggests that changes in PM_{2.5} during the resonance cycle were not the result of a single meteorological factor or socioeconomic factor. Future research on the issue of air pollution

prevention and control is crucial. We should pay more attention to the interaction between influencing factors on PM_{2.5}, as it elucidates the response relationship of PM_{2.5} concentration from a more comprehensive and scientific perspective.

5.3. Individual and synergistic effects of different socioeconomic factors on PM_{2.5}

The fourth finding was that PD, LUCC, INGDP, and EGDP had a positive contribution to PM_{2.5} while DEM had the opposite. This result is consistent with Yan et al. (2020) and Cheng et al. (2017), who estimated a significant positive role of PD in driving PM_{2.5} concentration through the scale and aggregation effect. The result, however, is different from the results of Yan et al. (2021), who obtained that PD in some cities helps alleviate PM_{2.5} pollution. The correlation between PD and PM_{2.5} was mainly due to overcrowding in the city, which led to an increase in demand for housing, public infrastructure, and transportation, causing an increase in urban resources and energy consumption. Meanwhile, a large amount of construction dust, industrial dust, fly ash, soot, and other disposable particulate pollutants were generated (Guo et al., 2021). Additionally, high PD areas are also not favorable for the dispersion of PM_{2.5} levels, which contributes indirectly to air pollution (Ouyang et al., 2021).

The reason for the relationship between LUCC and PM_{2.5} was that the excessive concentration of production factors produced a “crowding effect”, leading to higher land prices in urban centers and increasing production costs for enterprises, forcing commercial, residential, and industrial land to be transferred and expanded to the peripheral areas of the city. With the expansion of urban industrial land and the need to decentralize urban functions, urban space spread out in a disorderly manner (Guo et al., 2021). On the one hand, the increase in urban construction land means a relative reduction in the proportion of arable land, woodland, wetlands, and other ecological green areas, and the functional conversion of existing land uses results in a weakening of the service function of urban ecosystems for a certain period, and a decrease in their ecological restoration capacity and the purification function of pollutants (Zhu et al., 2019); on the other hand, the continued spatial expansion of cities has further led to the fragmentation of urban form and layout, relatively prolonging the commuting time of residents and increasing the total amount of solid particulate emissions due to a large number of private vehicles, which definitely affects the sustainable development of resources and the environment (Guo et al., 2021). Our results are inconsistent with the findings of Ouyang et al. (2021), who suggest that increased fragmentation can reduce urban PM_{2.5} emissions, essentially because fragmentation can improve the integration of urban land and urban forests. However, it is undeniable that through scientific planning and rational layout, and the protection of regional spatial development, it is possible to form an urban spatial structure of an appropriate scale, thus bringing into play the spatially concentrated scale effect of population and industry and reducing the PM_{2.5} concentration per unit land area (Yang et al., 2020).

Previous research argued that there is a positive correlation between PM_{2.5} and EGDP (Huang et al., 2019). This result was consistent with the results of this study. This also accords with earlier observations, which showed that energy intensity has a positive impact on haze pollution due to increases in energy intensity will increase electricity consumption (Cheng et al., 2017). Xi'an uses coal as its main energy source. In 2011, Xi'an consumed a total of 7.548 million tons of raw coal, with raw coal consumption accounting for over 80% of energy consumption (Cao, 2014). In the early years, most companies downplayed the development of clean coal technologies and put them into use (Xu et al., 2016). PD became larger and residential energy consumption came mainly from highly polluting coal, resulting in a growing EGDP, which also contributed to a rapid increase in PM_{2.5} emissions. However, energy prices have risen significantly and government environmental regulations have become stricter, resulting in an optimized energy consumption mix (Ji et al., 2018). The total natural gas supply increased from 53,202 (1000 cu.m) in 2005 to 285,215 (1000 cu.m) in 2018.⁵

Therefore, the impact of EGDP on PM_{2.5} emissions declined in later years. Studies have shown that energy activities in the industrial sector play a key role in PM_{2.5} emissions; therefore, INGDP is linked to energy activities (Yan et al., 2020). Total electricity consumption is used to designate energy consumption and the greater the electricity consumption is, the greater the electricity supply and the greater the PM_{2.5} emissions from coal-fired power plants (Yan et al., 2020).

A low PM_{2.5} concentration is usually accompanied by a high DEM value. Xi'an may trap pollutants at low altitudes, causing serious pollution at low altitudes. A similar study was also conducted by Yang (Yang et al., 2020). In terms of human activities, the terrain is an important limiting factor for population distribution and economic development (Zhang et al., 2019); human activities are mainly concentrated in low-lying areas, so pollutant emissions are usually plain-oriented (Huang et al., 2019). Tall terrain not only blocks airflow; areas with large undulations are also prone to forming special wind temperature fields and turbulence fields, which have a significant impact on the transmission, accumulation, diffusion, and settlement of PM_{2.5} (Huang et al., 2021). This also accords with earlier observations, which showed that due to the western Tibetan Plateau, there is a lack of air movement and the air masses encounter obstacles when moving out from the Sichuan Basin, and caused air pollution (Zhao et al., 2018).

We identified a negative influence of GDPPC on PM_{2.5} concentrations. This outcome was contrary to that of Wang who found that there was an inverted U-shaped relationship between GDPPC and PM_{2.5} concentrations (Wang et al., 2017). A possible explanation for this is that Xi'an has entered a post-industrial society, the industrial structure has been upgraded, clean energy and information technology have been widely used, and industrial exhaust emissions have been reduced (Wang and Fang, 2016). We identified that INGDP positively affects PM_{2.5} concentrations. Xi'an experienced a rapid industrialization process, and the impact of urbanization on the environment rose rapidly. This result was also similar to previous research (Wu et al., 2021). Previous studies have also suggested that higher GDP per capita leads to greater environmental awareness, which might conversely reduce PM_{2.5} concentrations (Zhou et al., 2018). The increase in the share of the secondary industry has significantly exacerbated urban haze pollution. Xi'an is in a phase of accelerated industrialization and urbanization, and the energy consumption of the secondary industry is much higher than that of other industries. Industrial production relies heavily on coal, and the large amount of pollutants generated by coal consumption directly contributes to haze pollution. Moreover, the prosperity of Xi'an's real estate industry relies on the sustainable development of the construction industry, which has largely driven the rapid development of heavy industries such as steel and cement.

The fifth finding was that the relationship between PM_{2.5} and GDP is phased. This is explained by the fact that (2000~2011) Xi'an experienced rapid economic development, high investment, and high pollution, which increased GDP with a huge environmental cost; the crude development model at the expense of the ecological environment has overwhelmed the ecological carrying threshold of the city, placing substantial pressure on resources and the environment, and causing the PM_{2.5} concentration to increase significantly. From 2012~2018, the impact of GDP gradually weakened. This stage of high-quality economic development and advanced industrial structure for industrial green development has the advantage of capital accumulation and technological innovation, forcing and boosting economic restructuring and transformation, and addressing the economic and social development dilemma with green production methods (Xie et al., 2016). Meanwhile, the agglomeration economy and positive externalities of green industries at this stage have enhanced the efficiency of centralized treatment of PM_{2.5} pollution sources (Guo et al., 2021). According to the Xi'an Statistical Yearbooks, annual electricity consumption increased

⁵ The source of its website is <https://tjj.xa.gov.cn/tjnj/2019/zk/indexch.htm>.

from 1482896 (10000 kWh) to 3967465 (10000 kWh), and possession of civil vehicles increased from 54.46 (10000 units) to 325.63(10000 units) in 2005~2018.⁶ Thus, it is necessary to further promote new energy vehicles in Xi'an. Similar to our results, a study suggests that economic development can decrease the PM_{2.5} concentration in lower quantile cities in 2013 ~ 2018 (Yan et al., 2020).

The sixth finding was that LUCC has high coupling with other factors and is a key parameter for PM_{2.5} control. A finding was also reported that population growth and LUCC in the process of urbanization will cause greater emissions of SO₂, NOx, and dust, which will increase PM_{2.5} concentrations (Wang and Fang, 2016). We also found a coupling effect of EGDP and other factors on PM_{2.5} throughout the study period; the increase in the proportion of Xi'an's secondary industry from 2004 to 2018 significantly aggravated urban smog pollution. This may be because of the higher PD when land is converted to artificial land in LUCC, with corresponding values of lower NDVI and higher energy use (EGDP), ultimately leading to higher PM_{2.5} concentrations; in contrast, the PM_{2.5} concentration decreased when the artificial land changed to natural land (Yang and Jiang, 2020). A previous study found that LUCC and NSL can effectively describe socioeconomic activity and urbanization (Wang et al., 2020). We found that the LUCC and NSL coupling factors had a progressively lower impact on PM_{2.5}. In the same way, the empirical results from Mi et al. (2021) confirmed that urbanization with more population density and traffic consuming more fossil fuels has caused high levels of PM_{2.5} pollution in Liaocheng, Puyang. The result of our study was due to the dramatic increase in population in Xi'an during the early years of urbanization, which eventually led to rapid real estate development in the city (Xu et al., 2016). For example, real estate investment increased from RMB 16.967 billion in 2004 to RMB 128.190 billion in 2012.⁷ When other sites in the LUCC were converted to housing construction large amounts of dust were generated, and dust is an important element in the formation of PM_{2.5} (Wang and Fang, 2016). Thus, urbanization causes LUCC to become a large-scale construction activity that generates large amounts of PM_{2.5}. However, worsening air pollution and increased environmental awareness have forced the government to enact reasonable measures to reduce dust pollution from real estate construction (Ji et al., 2018). For example, the vegetation cover of construction sites has increased. This also explains the cyclical effect of NSL on PM_{2.5}.

5.4. Limitations in this research

This paper examines the potential drivers of PM_{2.5} concentrations, but there are still many issues to be addressed. While the accuracy of the estimates based on PM_{2.5} satellite grid data is fairly presented, there is some uncertainty in different regions. Although all meteorological factors are resampled, their spatial resolution is slightly lower than that of other factors, which may affect the results of the paper. Therefore, to improve the precision of quantifying the anthropogenic contribution to PM_{2.5} pollution, further high spatial resolution emission inventory data will be adopted. The lack of a breakdown of the effect of LUCC on PM_{2.5} is also a shortcoming of this paper, and future studies will comprehensively analyze the effect of LUCC on PM_{2.5}.

5.5. Implications

(1) The above findings have major implications. There are significant regional differences in PM_{2.5} concentrations in Xi'an, thus it is necessary to adhere to the principle of 'local adaptation' in formulating environmental protection and ecological restoration policies and to avoid a 'one-size-fits-all' approach to policy formulation. The significant spatial autocorrelation of PM_{2.5} concentrations at Xi'an provides evidence for

the prevention and control of air pollution at regional levels that incorporate surrounding cities. Building a sense of "integration" is thus conducive to enhancing joint prevention and control of regional air pollution. The migration trajectory of the center of gravity of PM_{2.5} concentrations in Xi'an is generally shifted from the northeast to the southwest, indicating that the resource consumption constraint in the southwest of Xi'an is small, and the crude use of resources may have exacerbated PM_{2.5} concentrations in the region, which demonstrates the importance of decoupling economic growth and energy intensity. In the future, technological progress effects should be used to strengthen the key aspects of the scale of energy consumption and further increase the proportion of clean energy in the end-use energy consumption in the region (Guo et al., 2021).

(2) Given the continuous growth of PD and POP in Xi'an, the scientific formulation of a national land spatial development plan facilitates a rational spatial layout of the population. While the coupling effect of PD, POPs, and other socioeconomic factors on PM_{2.5} is relatively weak, the combined effect should not be overlooked. The advancement of urbanization will lead to an increase in urban POP and PD. With urban development, the increase in PD brings about agglomeration effects; the agglomeration effect improves the efficiency of public transport and resource use while encouraging shared pollution control facilities and reducing pollutant emissions. We argue that the positive externalities of the agglomeration effect have not yet been fully exploited, but that the scale effect has advantages. This requires Xi'an to make full use of the agglomeration effect in its urbanization process so that the positive externalities of resources and environmental benefits are fully utilized (Cheng et al., 2017).

(3) The proportion of new and green energy sources for heating should be increased. Compared with other seasons, heating played an important role in reducing PM_{2.5} concentration in winter. Therefore, there is a need to strengthen PM_{2.5} emission reduction measures for all heating enterprises. Moreover, we believe that energy efficiency improvements are still necessary. High energy efficiency stems from an advanced level of technological development, and companies should be encouraged to promote technologies for energy efficiency, energy storage, and efficient use of energy.

6. Conclusions

Based on remote sensing and GIS techniques, spatiotemporal variation and the driving factors of PM_{2.5} in Xi'an were examined at the city level. The results are as follows:

- (1) Between 2004 and 2018, concentrations of PM_{2.5} appeared obvious spatiotemporal heterogeneity over Xi'an and showed a trend upward initially and then downward. PM_{2.5} concentrations were highest in winter, followed by autumn, and lowest in summer. The main distribution of PM_{2.5} concentrations was significantly arranged in a northeast-southwest direction. The PM_{2.5} concentrations at Xi'an exhibited obvious spatial autocorrelation and spatial aggregation characteristics.
- (2) WTC indicated that U wind and LUCC have a strong impact on PM_{2.5}. PD, LUCC, INGDP, and EGDP presented a positive correlation with PM_{2.5} while DEM showed the opposite. Importantly, GDP showed different correlations across cycles. The coupled influence of Tem and RH had a strong influence on PM_{2.5} concentrations before 2011, followed by Tem and Pre, and Pre and RH dominated after 2011. Moreover, the interaction effect of LUCC and other factors had a greater influence on PM_{2.5} concentrations, while PD and POP with other factors displayed a smaller influence.

⁶ The source of its website is <https://tjj.xa.gov.cn/tjsj/tjxx/list/25.html>.

⁷ The source of its website is <https://tjj.xa.gov.cn/tjnj/2019/zk/indexch.htm>.

CRediT authorship contribution statement

Abula Tuheti: Conceptualization, Software, Validation, Formal analysis, Investigation, Resources, Data curation, Writing – original draft, Writing – review & editing, Visualization. **Shunxi Deng:** Writing – review & editing, Supervision, Project administration, Funding acquisition. **Jianghao Li:** Validation, Supervision. **Guanghua Li:** Validation, Supervision. **Pan Lu:** Visualization. **Zhenzhen Lu:** Validation. **Jiayao Liu:** Data curation. **Chenhui Du:** Visualization. **Wei Wang:** Formal analysis, Visualization.

Declaration of Competing Interest

The authors declare that they have no known competing financial interests or personal relationships that could have appeared to influence the work reported in this paper.

Data availability

We have provided data source websites in the paper

Acknowledgments:

The authors gratefully acknowledge that NASA provided the MODIS, TRMM satellite, NSL, and DEM data. ERA5 provides the meteorological data. The Landscan and Worldpop provide the PD and Pop data, respectively. The authors also acknowledge that CNLUCC provides the LUCC and ST data. Xi'an Statistical Yearbook provides the socio-economic indicators data.

This work was funded by the Key Research and Development Project of Shaanxi Province (No. 2021ZDLSF-05-07).

Appendix A. Supplementary data

Supplementary data to this article can be found online at <https://doi.org/10.1016/j.ecolind.2022.109802>.

References:

- Amantai, N., Ding, J., Ge, X., Bao, Q., 2021. Variation characteristics of actual evapotranspiration and meteorological elements in the Ebinur Lake basin from 1960 to 2017. *Acta Geograph. Sin.* 76, 1177–1192.
- Bari, M.A., Kindzierski, W.B., 2016. Fine particulate matter ($PM_{2.5}$) in Edmonton, Canada: source apportionment and potential risk for human health. *Environ. Pollut.* 218, 219–229.
- Cao, J., 2014. $PM_{2.5}$ and the environment in China. Science Press 2014: 115–116.
- Casallas, A., Castillo-Camacho, M.P., Guevara-Luna, M.A., González, Y., Sanchez, E., Belalcazar, L.C., 2022. Spatio-temporal analysis of $PM_{2.5}$ and policies in Northwestern South America. *Sci. Total Environ.* 852, 158504.
- Cheng, Z., Li, L., Liu, J., 2017. Identifying the spatial effects and driving factors of urban $PM_{2.5}$ pollution in China. *Ecol. Ind.* 82, 61–75.
- Chu, L., Huang, C., Liu, Q.S., Cai, C.F., Liu, C.H., 2020. Spatial heterogeneity of winter wheat yield and its determinants in the Yellow River Delta, China. *Sustainability* 12, 135–156.
- Csvaina, J., Field, J., Félix, O., Corral-Avilia, A.Y., Sáez, A.E., Betterton, E.A., 2014. Effect of wind speed and relative humidity on atmospheric dust concentrations in semi-arid climates. *Sci. Total Environ.* 487, 82–90.
- Dong, J., Liu, P., Song, H., Yang, D., Yang, J., Song, G., Miao, C., Zhang, J., Zhang, L., 2022. Effects of anthropogenic precursor emissions and meteorological conditions on $PM_{2.5}$ concentrations over the “2+26” cities of northern China. *Environ. Pollut.* 315, 120392.
- Du, Q., Zhou, J., Pan, T., Sun, Q., Wu, M., 2019. Relationship of carbon emissions and economic growth in China's construction industry. *J. Clean. Prod.* 220, 99–109.
- Duan, W., Wang, X., Cheng, S., Wang, R., 2022. Regional division and influencing mechanisms for the collaborative control of $PM_{2.5}$ and O_3 in China: A joint application of multiple mathematical models and data mining technologies. *J. Clean. Prod.* 337, 130607.
- Guang, W.u., Li, L.-J., Xiang, R.-B., 2019. $PM_{2.5}$ and its ionic components at a roadside site in Wuhan, China. *Atmos. Pollut. Res.* 10 (1), 162–167.
- Guo, X., Mu, X., Ding, Z., Qin, D., 2021. Nonlinear effects and driving mechanism of multidimensional urbanization on $PM_{2.5}$ concentrations in the Yangtze River Delta. *Acta Geograph. Sin.* 76, 1274–1293.
- He, Q., Geng, F., Li, C., Mu, H., Zhou, G., Liu, X., Gao, W., Wang, Y., Cheng, T., 2018. Long-term variation of satellite-based $PM_{2.5}$ and influence factors over East China. *Sci. Rep.* 8 (1).
- Hogrefe, C., 2012. Emissions versus climate change. *Nature Geosci.* 5 (10), 685–686.
- Hu, S., Yang, D., Qiu, H., Pei, Y., Song, J., Ma, S., et al., 2017. Influencing mechanisms of climate change on runoff process in the north slope of Qinling Mountains: a case of the Bahe River Basin. *Arid Land Geography* 40, 967–978.
- Huang, X., Shao, T., Jing-bo, C.J., Song, Y., 2019. Influence factors and spillover effect of $PM_{2.5}$ concentration on Fen-wei Plain. *China Environ. Sci.* 39, 3539–3548.
- Huang, X., Zhao, J., Cao, J., Xin, W., 2020. Evolution of the distribution of $PM_{2.5}$ concentration in the yangtze river economic belt and its influencing factors. *Environ. Sci.* 41, 1013–1024.
- Huang, X., Zhao, J., Sun, C., Tang, H., Liang, X., 2021. Orographic influences on the spatial distribution of $PM_{2.5}$ on the Fen-Wei Plain. *Environ. Sci.* 42, 4582–4592.
- Hudgins, L., Huang, J., 1996. Bivariate wavelet analysis of Asia Monsoon and Enso. *Adv. Atmos. Sci.* 13 (3), 299–312.
- Ji, X., Yao, Y., Long, X., 2018. What causes $PM_{2.5}$ pollution? Cross-economy empirical analysis from socioeconomic perspective. *Energy Policy* 119, 458–472.
- Jing, Z.Y., Liu, P.F., Wang, T.H., Song, H.Q., Lee, J., Xu, T., et al., 2020. Effects of meteorological factors and anthropogenic precursors on $PM_{2.5}$ concentrations in cities in China. *Sustainability* 12, 3350–3363.
- Lefever, D.W., 1926. Measuring geographic concentration by means of the Standard Deviations Ellipse. *Am. J. Sociol.* 32 (1), 88–94.
- Li, R., Li, Z., Gao, W., Ding, W., Xu, Q., Song, X., 2015. Diurnal, seasonal, and spatial variation of $PM_{2.5}$ in Beijing. *Sci. Bull.* 60 (3), 387–395.
- Li, R., Cui, L., Li, J., Zhao, A.N., Fu, H., Wu, Y.u., Zhang, L., Kong, L., Chen, J., 2017. Spatial and temporal variation of particulate matter and gaseous pollutants in China during 2014–2016. *Atmos. Environ.* 161, 235–246.
- Li, L., Qian, J., Ou, C.Q., Zhou, Y.X., Guo, C., Guo, Y., 2014. Spatial and temporal analysis of Air Pollution Index and its timescale-dependent relationship with meteorological factors in Guangzhou, China, 2001–2011. *Environ. Pollut.* 190, 75–81.
- Li, R., Wang, Z., Cui, L., Fu, H., Zhang, L., Kong, L., Chen, W., Chen, J., 2019. Air pollution characteristics in China during 2015–2016: spatiotemporal variations and key meteorological factors. *Sci. Total Environ.* 648, 902–915.
- Ling, W., Yang, Z., Qiang, L., Song, J., 2020. Study on spatial variation of China's territorial ecological space based on standard deviation ellipse. *Ecological Economy* 36, 176–181.
- Liu, Y., Li, Y., Chen, C., 2015. Pollution build on success in China. *Nature* 517 (7533), 145.
- Liu, Q., Wang, S., Zhang, W., Li, J., Dong, G., 2019. The effect of natural and anthropogenic factors on $PM_{2.5}$: empirical evidence from Chinese cities with different income levels. *Sci. Total Environ.* 653, 157–167.
- Londoño Pineda, A.A., Cano, J.A., 2021. Assessment of air quality in the Aburrá Valley (Colombia) using composite indices: Towards comprehensive sustainable development planning. *Urban Clim.* 39, 100942.
- Lu, X., Lin, C., Li, Y., Yao, T., Fung, J.C., Lau, A.K., 2017b. Assessment of health burden caused by particulate matter in southern China using high-resolution satellite observation. *Environ. Int.* 98, 160–170.
- Lu, D., Xu, J., Yang, D., Zhao, J., 2017a. Spatio-temporal variation and influence factors of $PM_{2.5}$ concentrations in China from 1998 to 2014. *Atmos. Pollut. Res.* 8 (6), 1151–1159.
- Lv, B., Zhang, B., Bai, Y., 2016. A systematic analysis of $PM_{2.5}$ in Beijing and its sources from 2000 to 2012. *Atmos. Environ.* 2016 (124), 98–108.
- Masiol, M., Hopke, P.K., Felton, H.D., Frank, B.P., Rattigan, O.V., Wurth, M.J., LaDuke, G.H., 2016. Source apportionment of $PM_{2.5}$ chemically speciated mass and particle number concentrations in New York city. *Atmos. Environ.* 148, 215–229.
- Mateus-Fon tech, L., Vargas-Burbano, A., Jimenez, R., Rojas, N.Y., Rueda-Saa, G., van Pinxteren, D., van Pinxteren, M., Fomba, K.W., Herrmann, H., 2022. Understanding aerosol composition in a tropical inter-Andean valley impacted by agro-industrial and urban emissions. *Atmos. Chem. Phys.* 22 (13), 8473–8495.
- Meng, C., Cheng, T., Gu, X., Shi, S., Wang, W., Wu, Y.u., Bao, F., 2019. Contribution of meteorological factors to particulate pollution during winters in Beijing. *Sci. Total Environ.* 656, 977–985.
- Mi, Y., Sun, K., Li, L.i., Lei, Y., Wu, S., Tang, W., Wang, Y., Yang, J., 2021. Spatiotemporal pattern analysis of $PM_{2.5}$ and the driving factors in the middle Yellow River urban agglomerations. *J. Clean. Prod.* 299, 126904.
- Niu, X., Cao, J., Shen, Z., Ho, S.S.H., Tie, X., Zhao, S., Xu, H., Zhang, T., Huang, R., 2016. $PM_{2.5}$ from the Guanzhong Plain: Chemical composition and implications for emission reductions. *Atmos. Environ.* 147, 458–469.
- Ouyang, X., Wei, X., Li, Y., Wang, X.-C., Kleme, J., 2021. Impacts of urban land morphology on $PM_{2.5}$ concentration in the urban agglomerations of China. *J. Environ. Manage.* 283, 112000–112011.
- Rodríguez-Gómez, C., Echeverry, G., Jaramillo, A., Ladino, L.A., 2021. The negative impact of biomass burning and the Orinoco low-level jet on the air quality of the Orinoco River Basin. *Atmósfera*.
- Rupakheti, D., Yin, X., Rupakheti, M., Zhang, Q., Li, P., Rai, M., Kang, S., 2021. Spatio-temporal characteristics of air pollutants over Xinjiang, northwestern China. *Environ. Pollut.* 268, 115907.
- Shi, K., Wu, Y., Li, L., 2021. Quantifying and evaluating the effect of urban expansion on the fine particulate matter ($PM_{2.5}$) emissions from fossil fuel combustion in China. *Ecol. Ind.* 125, 107541–107551.
- Song, Y., Wang, X., Maher, B.A., Li, F., Xu, C., Liu, X., Sun, X., Zhang, Z., 2016. The spatial-temporal characteristics and health impacts of ambient fine particulate matter in China. *J. Clean. Prod.* 112, 1312–1318.
- Sun, T., Zhang, T., Xiang, Y., Fan, G., Fu, Y., Lv, L., Zheng, H., 2022. Application of data assimilation technology in source apportionment of $PM_{2.5}$ during winter haze

- episodes in the Beijing-Tianjin-Hebei region in China. *Atmos. Pollut. Res.* 13 (10), 101546.
- van Donkelaar, A., Martin, R.V., Brauer, M., Hsu, N.C., Kahn, R.A., Levy, R.C., Lyapustin, A., Sayer, A.M., Winker, D.M., 2016. Global estimates of fine particulate matter using a combined geophysical-statistical method with information from satellites, models, and monitors. *Environ. Sci. Tech.* 50 (7), 3762–3772.
- Wang, Z.B., Fang, C.L., 2016. Spatial-temporal characteristics and determinants of PM_{2.5} in the Bohai Rim urban agglomeration. *Chemosphere* 148, 148–162.
- Wang, D., Hu, J., Xu, Y., Lv, D.I., Xie, X., Kleeman, M., Xing, J., Zhang, H., Ying, Q.i., 2014. Source contributions to primary and secondary inorganic particulate matter during a severe wintertime PM_{2.5} pollution episode in Xi'an, China. *Atmos. Environ.* 97, 182–194.
- Wang, W., Samat, A., Abduwaili, J., Ge, Y., 2020. Spatio-temporal variations of satellite-based PM_{2.5} concentrations and its determinants in Xinjiang, Northwest of China. *Int. J. Environ. Res. Public Health* 17, 2157–2181.
- Wang, J., Xu, C., 2017. Geodetector: principle and prospective. *Acta Geograph. Sin.* 72, 116–134.
- Wang, S., Zhou, C., Wang, Z., Feng, K., Hubacek, K., 2017. The characteristics and drivers of fine particulate matter (PM_{2.5}) distribution in China. *J. Clean. Prod.* 142, 1800–1809.
- Wu, Q., Guo, R., Luo, J., Chen, C., 2021. Spatiotemporal evolution and the driving factors of PM_{2.5} in Chinese urban agglomerations between 2000 and 2017. *Ecol. Ind.* 125, 107491–107504.
- Xie, R., Sabel, C.E., Lu, X.i., Zhu, W., Kan, H., Nielsen, C.P., Wang, H., 2016. Long-term trend and spatial pattern of PM_{2.5} induced premature mortality in China. *Environ. Int.* 97, 180–186.
- Xu, P., Ju, H., Ji, D., Zhang, J., Yue, Z., Hu, B., et al., 2014. Observation of atmospheric pollutants in the urban area of beibei district, Chongqing. *Environ. Sci.* 35, 820–828.
- Xu, B., Luo, L., Lin, B., 2016. A dynamic analysis of air pollution emissions in China: Evidence from nonparametric additive regression models. *Ecol. Ind.* 63, 346–358.
- Xu, G., Yan, L., Hong, Y., Guo, H., 2015. Analysis on spatial-temporal characteristics and driving factors of PM_{2.5} in Henan province from 2015 to 2019. *Environ. Sci.* 2022 (43), 1697–1705.
- Yan, D., Lei, Y., Shi, Y., Zhu, Q., Li, L., Zhang, Z., 2018. Evolution of the spatiotemporal pattern of PM_{2.5} concentrations in China-A case study from the Beijing-Tianjin-Hebei region. *Atmos. Environ.* 183, 225–233.
- Yan, D., Ren, X., Kong, Y., Ye, B., Liao, Z., 2020. The heterogeneous effects of socioeconomic determinants on PM_{2.5} concentrations using a two-step panel quantile regression. *Appl. Energy* 272, 115246.
- Yan, D., Kong, Y., Jiang, P., Huang, R., Ye, B., 2021. How do socioeconomic factors influence urban PM_{2.5} pollution in China? Empirical analysis from the perspective of spatiotemporal disequilibrium. *Sci. Total Environ.* 761, 143266–143279.
- Yang, W., Jiang, X., 2020. Interannual characteristics of fine particulate matter in north China and its relationship with land use and land cover change. *Environ. Sci.* 41, 2995–3003.
- Yang, D., Wang, X., Xu, J., Xu, C., Lu, D., Ye, C., Wang, Z., Bai, L., 2018. Quantifying the influence of natural and socioeconomic factors and their interactive impact on PM_{2.5} pollution in China. *Environ. Pollut.* 241, 475–483.
- Yang, Q., Yuan, Q., Yue, L., Li, T., 2020. by using modified geographically weighted regression. *Environ. Pollut.* 262, 114257.
- Zhang, L., An, J.i., Liu, M., Li, Z., Liu, Y., Tao, L., Liu, X., Zhang, F., Zheng, D., Gao, Q.i., Guo, X., Luo, Y., 2020a. Spatiotemporal variations and influencing factors of PM_{2.5} concentrations in Beijing, China. *Environ. Pollut.* 262, 114276.
- Zhang, X.X., Xu, C.D., Xiao, G.X., 2020b. Spatial heterogeneity of the association between temperature and hand, foot, and mouth disease risk in metropolitan and other areas. *Sci. Total Environ.* 713, 136623–136629.
- Zhang, X., Xu, H., Liang, D., 2022. Spatiotemporal variations and connections of single and multiple meteorological factors on PM_{2.5} concentrations in Xi'an, China. *Atmos. Environ.* 275, 119015.
- Zhang, J., Zhu, W., Zhu, L., Cui, Y., He, S., Ren, H., 2019. Topographical relief characteristics and its impact on population and economy: a case study of the mountainous area in western Henan, China. *J. Geogr. Sci.* 29 (4), 598–612.
- Zhao, S., Yu, Y., Yin, D., Qin, D., He, J., Dong, L., 2018. Spatial patterns and temporal variations of six criteria air pollutants during 2015 to 2017 in the city clusters of Sichuan Basin, China. *Sci. Total Environ.* 624, 540–557.
- Zhao, R., Zhan, L., Yao, M., Yang, L., 2020. A geographically weighted regression model augmented by Geodetector analysis and principal component analysis for the spatial distribution of PM_{2.5}. *Sustain. Cities Soc.* 56, 102106.
- Zhao, X., Zhou, W., Han, L., Locke, D., 2019. Spatiotemporal variation in PM_{2.5} concentrations and their relationship with socioeconomic factors in China's major cities. *Environ. Int.* 133, 105145.
- Zhou, C., Chen, J., Wang, S., 2018. Examining the effects of socioeconomic development on fine particulate matter (PM_{2.5}) in China's cities using spatial regression and the geographical detector technique. *Sci. Total Environ.* 619–620, 436–445.
- Zhu, W., Xu, X., Zheng, J., Yan, P., Wang, Y., Cai, W., 2018. The characteristics of abnormal wintertime pollution events in the Jing-Jin-Ji region and its relationships with meteorological factors. *Sci. Total Environ.* 626, 887–898.
- Zhu, W., Wang, M., Zhang, B., 2019. The effects of urbanization on PM_{2.5} concentrations in China's Yangtze River Economic Belt: New evidence from spatial econometric analysis. *J. Clean. Prod.* 239, 118065.